

# Exhibit GG

## Exhibit D-21

**Invalidity of U.S. Patent No. 6,922,632 (“’632 Patent”) Under Pre-AIA Section 102 or Section 103 in view of Gregory Welch, SCAAT: Incremental Tracking with Incomplete Information (October 1996) (Ph.D. dissertation, Univ. of N.C. at Chapel Hill) (on file with Dept. of Comp. Sci., Univ. of N.C.) (“Welch Thesis”)<sup>1</sup>**

Welch Thesis was publicly available as early as than May 24, 1997. Plaintiffs belatedly asserted a priority date of June 13, 2001 for the ’632 Patent on December 22, 2021, 71 days after the Court’s deadline. Defendants have reviewed Plaintiffs’ alleged evidence of the purported June 13, 2001 priority date, and maintain that the ’632 Patent is not entitled to this priority date. *See* Defendants’ March 15, 2022 Supplemental Invalidity Contentions. Defendants reserve their objections to Plaintiffs’ belated assertion of the new priority date and expressly reserve all rights to challenge this alleged new priority date. As such, Defendants assume for the sake of these invalidity contentions, that the priority date for the ’632 Patent is August 9, 2002 based on the first filed Provisional Application from which the ’632 Patent claims priority. (Defendants do not concede nor agree that Plaintiffs are even entitled to this date.) Assuming this priority date, Welch Thesis qualifies as prior art under at least pre-AIA Sections 102 (a) and (b) to the ’632 Patent.

As described herein, the asserted claims of the ’632 Patent are invalid (a) under one or more sections of 35 U.S.C. § 102 as anticipated expressly or inherently by Welch Thesis (including the documents incorporated into Welch Thesis by reference), and (b) under 35 U.S.C. § 103 as obvious in view of Welch Thesis standing alone, and additionally, in combination with the knowledge of one of ordinary skill in the art, and/or other prior art, including but not limited to the prior art identified in Defendants’ Invalidity Contentions and the prior art described in the claim charts attached in Exhibits D-1 – D-22. With respect to the proposed modifications to Welch Thesis, as of the priority date of the ’632 Patent, such modification would have been obvious to try, an obvious combination of prior art elements according to known methods to yield predictable results, a simple substitution of one known element for another to obtain predictable results, a use of known techniques to improve a similar devices or method in the same way, an application of a known technique to a known device or method ready for improvement to yield predictable results, a variation of a known work in one field of endeavor for use in either the same field or a different one based on design incentives or other market forces with variations that are predictable to one of ordinary skill in the art, and/or obvious in view of teachings, suggestions, and motivations in the prior art that would have led one of ordinary skill to modify or combine the prior art references.

---

<sup>1</sup> Discovery in this case is ongoing and, accordingly, this invalidity chart is not to be considered final. Defendants have conducted the invalidity analysis herein without having fully undergone claim construction and a *Markman* hearing. By charting the prior art against the claim(s) herein, Defendants are not admitting nor agreeing to Plaintiffs’ interpretation of the claims at issue in this case. Additionally, these charts provide representative examples of portions of the charted references that disclose the indicated limitations under Plaintiffs’ application of the claims; additional portions of these references other than the representative examples provided herein may also disclose the indicated limitation(s) and Defendants contend that the asserted claim(s) are invalid in light of the charted reference(s) as a whole. Defendants reserve the right to rely on additional citations or sources of evidence that also may be applicable, or that may become applicable in light of claim construction, changes in Plaintiffs’ infringement contentions, and/or information obtained during discovery as the case progresses. Further, by submitting these invalidity contentions, Defendants do not waive and hereby expressly reserve their right to raise other invalidity defenses, including but not limited to defenses under Sections 101 and 112. Defendants reserve the right to amend or supplement this claim chart at a later date, including after the Court’s order construing disputed claim terms.

## Exhibit D-21

All cross-references should be understood to include material that is cross-referenced within the cross-reference. Where a particular figure is cited, the citation should be understood to encompass the caption and description of the figure as well as any text relating to or describing the figure. Conversely, where particular text referring to a figure is cited, the citation should be understood to include the figure as well.

## A. INDEPENDENT CLAIM 1

CLAIM 1	Welch Thesis
<p>[1.pre] A method for tracking an object comprising:</p>	<p>At least under Plaintiffs' apparent infringement theory, Welch Thesis discloses, either expressly or inherently, a method for tracking an object.</p> <p>No party has yet asserted that the preamble is limiting, nor has the Court construed the preamble as limiting. However, to the extent that the preamble is limiting, it is disclosed by Welch Thesis.</p> <p>In the alternative, this element would be obvious over Welch Thesis in light of the other references disclosed in Defendants' Invalidity Contentions and/or the knowledge of one of ordinary skill in the art.</p> <p><i>See, e.g.:</i></p> <p>The Kalman filter provides a powerful mathematical framework within which a minimum mean-square-error estimate of a user's position and orientation can be tracked using a sequence of single sensor observations, as opposed to groups of observations. We refer to this new approach as single-constraint-at-a-time or SCAAT tracking. <b>The method improves accuracy</b> by properly assimilating sequential observations, filtering sensor measurements, and by concurrently autocalibrating mechanical or electrical devices. <b>The method facilitates user motion prediction, multisensor data fusion, and in systems where the observations are only available sequentially it provides estimates at a higher rate and with lower latency than a multiple-constraint approach.</b></p> <p>Welch Thesis at Abstract.</p> <p>The most significant aspect of this work is the <b>introduction and exploration of the SCAAT approach to 3D tracking for virtual environments.</b> However I also believe that this work may prove to be of interest to the larger scientific and engineering community in addressing a more general class of tracking and estimation problems.</p> <p>Welch Thesis at Abstract.</p>

## Exhibit D-21

CLAIM 1	Welch Thesis
	<p><i>See also</i> Welch Thesis, Chapter 1.3 (describing how SCAAT is an “unusual approach to tracking”); Chapter 2.1 (describing the use of Kalman filters “in the context of tracking or navigation”); Chapter 4.3 (describing how the SCAAT algorithm is used for tracking); Chapter 7.7 (describing “other tracking implementations” for the SCAAT algorithm).</p> <p><i>See also</i> Defendants’ Invalidity Contentions for further discussion.</p>
<p>[1.a] coupling a sensor subsystem to an estimation subsystem, said sensor subsystem enabling measurement related to relative locations or orientations of sensing elements;</p>	<p>At least under Plaintiffs’ apparent infringement theory, Welch Thesis discloses, either expressly or inherently, coupling a sensor subsystem to an estimation subsystem, said sensor subsystem enabling measurement related to relative locations or orientations of sensing elements. In the alternative, this element would be obvious over Welch Thesis in light of the other references disclosed in Defendants’ Invalidity Contentions and/or the knowledge of one of ordinary skill in the art.</p> <p><i>See, e.g.:</i></p> <p><b>A Kalman filter can be used to estimate a globally-observable process by sequentially incorporating only measurements of locally-unobservable processes.</b> The use of a Kalman filter in such a manner offers several advantages: (1) a flexible framework for heterogeneous multisensor data fusion; (2) a unique opportunity to perform concurrent device autocalibration; and in a system that allows only sequential measurements, (3) significantly improved estimate rates and latencies; and (4) avoidance of the incorrect simultaneity assumption. Welch Thesis at 43</p> <p><b>The Kalman filter is a set of mathematical equations that provides an efficient computational (recursive) means of using noisy measurements to estimate the state of a linear system, while minimizing the expected mean-squared estimation error.</b> Welch Thesis at 45.</p> <p><b>The SCAAT method represents an unusual approach to Kalman filter based multisensor data fusion.</b> Because the filter operates on single sensor measurements, new estimates can be computed as soon as measurements from an individual sensor of any type become available, in virtually any order, and at any (possibly varying) rate. <b>Such flexibility allows measurements from any combination of devices to be interlaced in the most convenient and expeditious fashion, ensuring that each estimate is computed from the most recent data offered by any combination of devices. The information from the various observations can then be</b></p>

## Exhibit D-21

CLAIM 1	Welch Thesis
	<p><b>blended using either a single SCAAT KF with multiple measurement models, or separate SCAAT filters</b> (and thus statistics) each with single measurement models, in which case the estimates from the various models can be blended using a statistical multi-model approach (see for example [Bar-Shalom93]). Welch Thesis at 56-57.</p> <p>For the sake of illustration, <b>imagine an inertial-acoustical hybrid tracking system composed of three accelerometers, three rate gyros, and an acoustical line-of-sight system (to control drift from the inertial sensors).</b> Note that not only will the acoustical measurements take longer than the inertial measurements, the acoustical measurement times will vary with distance between the source and sensors. A conventional method for data fusion might repeat the fixed pattern shown in figure 2.7. Notice that an estimate is produced only after collecting an orthogonal group of measurements from each (any one) subsystem.</p> <div data-bbox="598 669 1012 852"> <p>The diagram illustrates a timing sequence over time. Accelerometers (red) and Rate Gyros (green) provide continuous, frequent measurements. Acoustic Ranging (blue) measurements are delayed and occur in groups of three (x, y, z). The Estimate (vertical bars) is updated only after each group of three homogeneous measurements.</p> </div> <p><b>Figure 2.7:</b> Timing diagram for a hypothetical conventional hybrid tracking system. The state estimate is updated only after each group of 3 homogeneous measurements.</p> <p>In contrast, a SCAAT implementation might interleave sensor measurements as depicted in figure 2.8. Note the flexibility of measurement type, availability, rate, and ordering. Again because an estimate is produced with every sensor measurement, latency is reduced and the estimation rate is increased.</p>

## Exhibit D-21

## CLAIM 1

## Welch Thesis

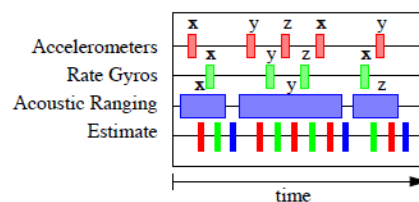


Figure 2.8: Timing diagram for a SCAAT inertial-acoustic hybrid tracking system. The state estimate is updated whenever an individual measurement becomes available.

Welch Thesis at 57.-58.

On the other hand, because the SCAAT method generates a new tracking estimate with each individual measurement, individual device imperfections are more readily identified. Furthermore, because the simultaneity assumption is avoided, the motion restrictions discussed in section 2.3.2 are removed, and autocalibration can be performed while concurrently tracking a target under normal conditions. The specific autocalibration method is presented in chapter 4, with experimental results in chapter 6.

Welch Thesis at 61

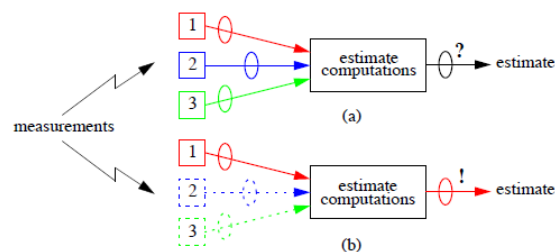
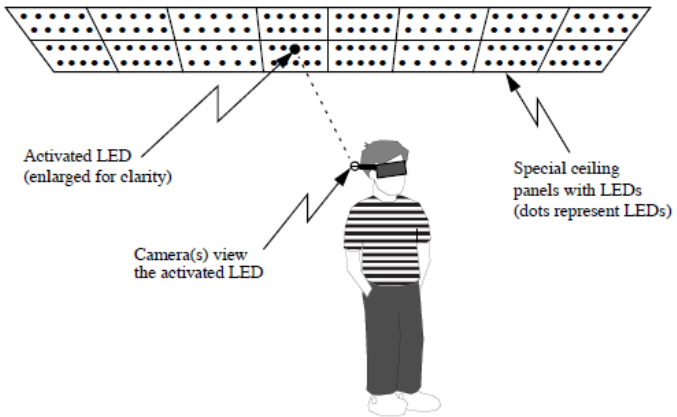


Figure 2.11: Autocalibration and attribution of measurement error. (a) Most algorithms operate on multiple measurements as a group, hence uncertainty or error (represented by the ellipses) in the final estimates is difficult to attribute to any individual sensor. (b) With the SCAAT method, uncertainty in final estimates can more easily be attributed to a particular individual sensor.

Welch Thesis at 62.

The tracking system that I employ in my experiments is an “inside-looking-out” optoelectronic system designed for interactive computer graphics or virtual environments. The system, which we call the “HiBall tracker”, is an improved version of the wide-area system described in [Ward92]. **In these systems, user-mounted optical**

## Exhibit D-21

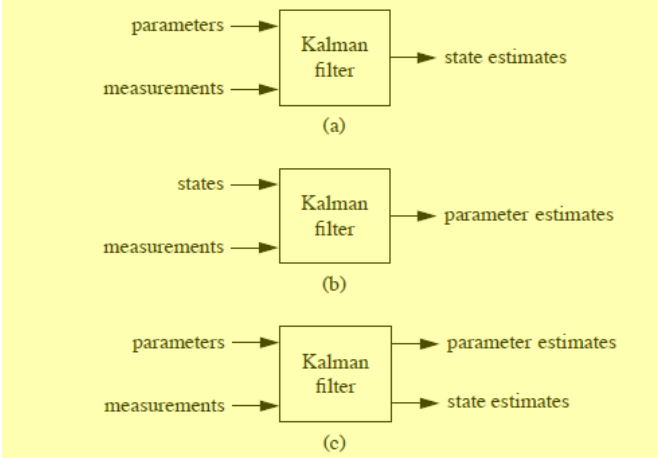
CLAIM 1	Welch Thesis
	<p><b>sensors observe infrared light-emitting diodes (LEDs) or beacons mounted in the ceiling above the user. The locations of the beacons are known (to some degree) so observations of them can be used to estimate the user's position and orientation.</b></p> <p>Welch Thesis at 191.</p>  <p><b>Figure D.1: An outward-looking optoelectronic tracking system. User-mounted cameras look outward (generally upward) at active beacons in the environment.</b></p> <p>Welch Thesis at 191.</p> <p>One goal of the HiBall system is to provide a user with <i>wide-area</i> tracking. To this end, the LEDs are installed in special ceiling panels that replace standard-size acoustic ceiling tiles. (See figure D.1.) These tiles can be installed over a large area, thus providing a large working area. In fact, the current UNC installation consists of enough ceiling tiles to cover an area of approximately 5x5 meters, with a corresponding total of over 3,000 LEDs. The LED positions in world coordinates are initially estimated based on the ceiling panel design, which has them installed in a regular two-dimensional grid.</p> <p>The LEDs are connected to special circuit boards that are mounted on (above) the ceiling tiles, and these circuit boards are then connected to a computer. Thus LEDs can be individually activated under computer control as needed for the SCAAT observations. (The ceiling circuitry allows beacon activation at over 5000 LEDs per second.)</p> <p>Welch Thesis at 192.</p>

## Exhibit D-21

CLAIM 1	Welch Thesis
	<p>In the original system described by [Ward92] the user wore a relatively large head-mounted mechanical fixture that supported several individually self-contained optical sensors or “cameras” and a backpack that contained the necessary signal processing and A/D conversion circuitry as shown in figure D.2.</p> <p>In the new system the camera fixture and backpack in figure D.2 are together replaced by a relatively small sensor cluster called the HiBall. Figure D.3 is a picture of an unpopulated HiBall with a golf ball to convey a notion of size.</p> <p>A populated HiBall contains six lenses, six photodiodes with infrared filters, and all of the necessary circuitry for signal processing, A/D conversion, control, and high-speed serial communication. It is designed so that each photodiode can view infrared beacons (LEDs in this case) through each of several adjacent lenses, thus implementing up to 26 distinct infrared cameras.</p> <p>The photodiodes provide four signals that together indicate the position of the centroid of light (infrared in this case) as it appears on the two-dimensional photodiode surface. At any point in time, the internal A/D conversion circuitry can sample these signals for any one photodiode. These samples would then be sent to an external computer via a high-speed serial link where they would be converted to the measurement that reflect the position of the image of the infrared beacon on the two-dimensional photodiode.</p> <p>If the photodiode measurements are viewed as images of the ceiling beacons (known scene points), the HiBall tracker can be viewed as an implementation of the abstract image-based example initially introduced in section 1.2 on page 39 (see figures 1.4-1.6) and later used in chapter 5. Hence my frequent references to a HiBall lens and sensor pair as a camera.</p> <p>Welch Thesis at 192-93.</p> <p><i>See also</i> Defendants’ Invalidity Contentions for further discussion.</p>
[1.b] accepting configuration data from the sensor subsystem;	<p>At least under Plaintiffs’ apparent infringement theory, Welch Thesis discloses, either expressly or inherently, accepting configuration data from the sensor subsystem. In the alternative, this element would be obvious over Welch Thesis in light of the other references disclosed in Defendants’ Invalidity Contentions and/or the knowledge of one of ordinary skill in the art.</p> <p><i>See, e.g.:</i></p>



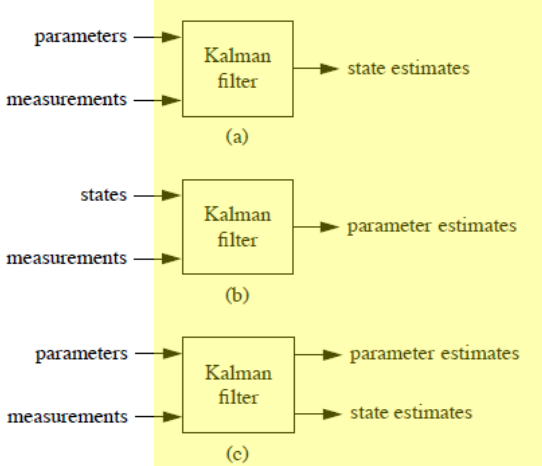
## Exhibit D-21

CLAIM 1	Welch Thesis
	 <p>Figure 2.2: State versus parameter estimation. (a) The system parameters are known, and are used with the measurements to estimate the states. (b) For calibration purposes, known states can be used with measurements to estimate the system parameters. (c) A set of parameters can be used in conjunction with measurements to estimate another (not necessarily disjoint) set of parameters <i>and</i> the states.</p> <p>Welch Thesis at 49.</p>

## Exhibit D-21

CLAIM 1	Welch Thesis
	<div data-bbox="510 248 1161 540"> <p>Figure 2.11 consists of two diagrams, (a) and (b). In (a), three measurements (1, 2, 3) are shown as colored boxes with arrows pointing to a single 'estimate computations' block. The output is an 'estimate' with a question mark in an ellipse. In (b), the same three measurements are shown, but measurement 2 is dashed and measurement 3 is dotted. The 'estimate computations' block outputs an 'estimate' with an exclamation mark in an ellipse, indicating attribution of error to a specific sensor.</p> </div> <p><b>Figure 2.11:</b> Autocalibration and attribution of measurement error. (a) Most algorithms operate on multiple measurements as a group, hence uncertainty or error (represented by the ellipses) in the final estimates is difficult to attribute to any individual sensor. (b) With the SCAAT method, uncertainty in final estimates can more easily be attributed to a particular individual sensor.</p> <p>Welch Thesis at 62.</p> <div data-bbox="653 784 1325 1198"> <p>Figure 4.12 is a flowchart showing a cycle between 'Time Update' and 'Measurement Update'. The 'Measurement Update' block is highlighted in yellow and contains three steps: 1. Augment with device parameters, 2. Main tracker algorithm, and 3. Extract device parameters. Arrows indicate a clockwise flow from Time Update to Measurement Update and back.</p> </div> <p><b>Figure 4.12:</b> The revised tracking algorithm for autocalibration. The time update consists of equation (4.14). The measurement update consists of equations (4.24)-(4.27), then (4.15)-(4.22), and finally equation (4.28).</p> <p>Welch Thesis at 102.</p> <p><i>See also</i> Welch Thesis Chapter 2.5 (describing autocalibration for sensor subsystems); Chapter 4.4 (autocalibration using SCAAT algorithm); Chapter 6.1 (describing autocalibration of HiBall sensor system using SCAAT)</p>

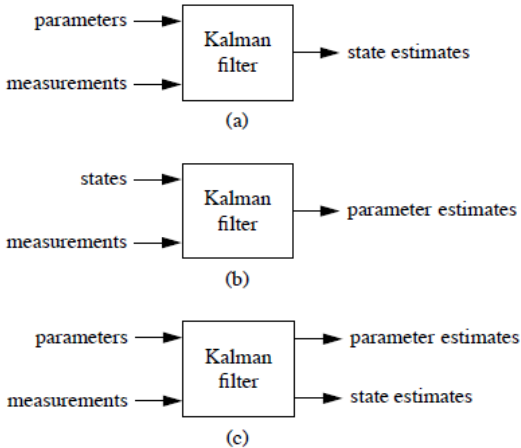
## Exhibit D-21

CLAIM 1	Welch Thesis
	<p><i>See also</i> Defendants' Invalidity Contentions for further discussion.</p>
<p>[1.c] configuring the estimation system according to the accepted configuration data;</p>	<p>At least under Plaintiffs' apparent infringement theory, Welch Thesis discloses, either expressly or inherently, configuring the estimation system according to the accepted configuration data. In the alternative, this element would be obvious over Welch Thesis in light of the other references disclosed in Defendants' Invalidity Contentions and/or the knowledge of one of ordinary skill in the art.</p> <p><i>See, e.g.:</i></p>  <p><b>Figure 2.2:</b> State versus parameter estimation. (a) The system parameters are known, and are used with the measurements to estimate the states. (b) For calibration purposes, known states can be used with measurements to estimate the system parameters. (c) A set of parameters can be used in conjunction with measurements to estimate another (not necessarily disjoint) set of parameters <i>and</i> the states.</p> <p>Welch Thesis at 49.</p>

## Exhibit D-21

CLAIM 1	Welch Thesis
	<div data-bbox="510 248 1161 540"> <p>Figure 2.11 consists of two diagrams, (a) and (b). In both, three measurements (1, 2, 3) are shown on the left, each with an associated uncertainty ellipse. Arrows from these measurements point to a box labeled 'estimate computations'. In (a), the arrows are solid and the output 'estimate' has a question mark in an ellipse. In (b), the arrows are dashed and the output 'estimate' has an exclamation mark in an ellipse, indicating attribution of error to a specific sensor.</p> </div> <p><b>Figure 2.11:</b> Autocalibration and attribution of measurement error. (a) Most algorithms operate on multiple measurements as a group, hence uncertainty or error (represented by the ellipses) in the final estimates is difficult to attribute to any individual sensor. (b) With the SCAAT method, uncertainty in final estimates can more easily be attributed to a particular individual sensor.</p> <p>Welch Thesis at 62.</p> <div data-bbox="653 784 1325 1198"> <p>Figure 4.12 is a flowchart showing a cycle between two main components: 'Time Update' and 'Measurement Update'. The 'Measurement Update' component is a large oval containing a numbered list: 1. Augment with device parameters, 2. Main tracker algorithm, 3. Extract device parameters. Arrows indicate a clockwise flow from 'Time Update' to 'Measurement Update' and back.</p> </div> <p><b>Figure 4.12:</b> The revised tracking algorithm for autocalibration. The time update consists of equation (4.14). The measurement update consists of equations (4.24)-(4.27), then (4.15)-(4.22), and finally equation (4.28).</p> <p>Welch Thesis at 102.</p> <p><i>See also</i> Welch Thesis Chapter 2.5 (describing autocalibration for sensor subsystems); Chapter 4.4 (autocalibration using SCAAT algorithm); Chapter 6.1 (describing autocalibration of HiBall sensor system using SCAAT)</p>

## Exhibit D-21

CLAIM 1	Welch Thesis
	<p><i>See also</i> Defendants' Invalidity Contentions for further discussion.</p>
<p>[1.d] repeatedly updating a state estimate, including accepting measurement information from the sensor subsystem, and updating the state estimate according to the accepted configuration data and the accepted measurement data.</p>	<p>At least under Plaintiffs' apparent infringement theory, Welch Thesis discloses, either expressly or inherently, repeatedly updating a state estimate, including accepting measurement information from the sensor subsystem, and updating the state estimate according to the accepted configuration data and the accepted measurement data. In the alternative, this element would be obvious over Welch Thesis in light of the other references disclosed in Defendants' Invalidity Contentions and/or the knowledge of one of ordinary skill in the art.</p> <p><i>See, e.g.:</i></p>  <p><b>Figure 2.2:</b> State versus parameter estimation. (a) The system parameters are known, and are used with the measurements to estimate the states. (b) For calibration purposes, known states can be used with measurements to estimate the system parameters. (c) A set of parameters can be used in conjunction with measurements to estimate another (not necessarily disjoint) set of parameters <i>and</i> the states.</p> <p>Welch Thesis at 49.</p>

## Exhibit D-21

## CLAIM 1

## Welch Thesis

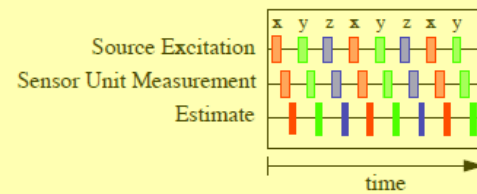


Figure 2.4: Timing diagram for a (hypothetical) SCAAT magnetic tracker. The state estimate is updated after sensing each individual excitation vector.

Welch Thesis at 52.

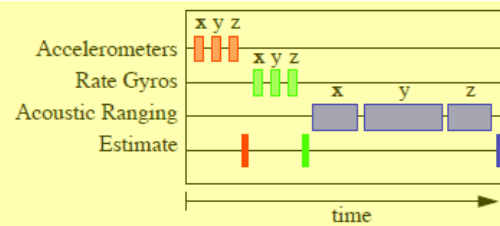


Figure 2.7: Timing diagram for a hypothetical conventional hybrid tracking system. The state estimate is updated only after each group of 3 homogeneous measurements.

Welch Thesis at 57.

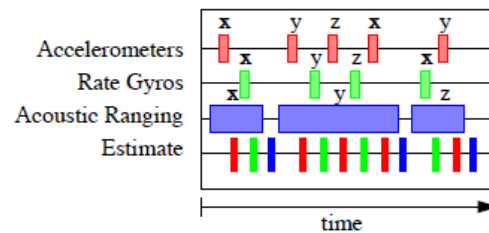
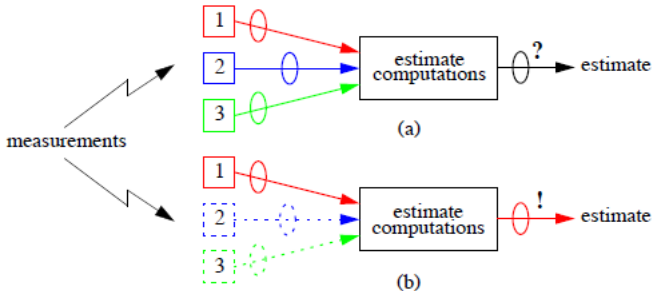


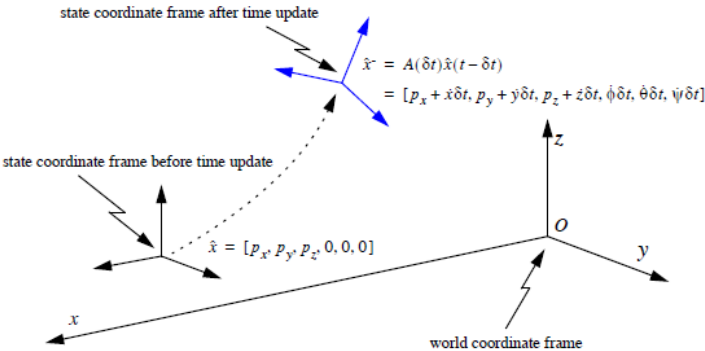
Figure 2.8: Timing diagram for a SCAAT inertial-acoustic hybrid tracking system. The state estimate is updated whenever an individual measurement becomes available.

Welch Thesis at 58.

Exhibit D-21

CLAIM 1	Welch Thesis
	<div data-bbox="514 248 1163 537"></div> <p data-bbox="527 553 1157 695"><b>Figure 2.11:</b> Autocalibration and attribution of measurement error. (a) Most algorithms operate on multiple measurements as a group, hence uncertainty or error (represented by the ellipses) in the final estimates is difficult to attribute to any individual sensor. (b) With the SCAAT method, uncertainty in final estimates can more easily be attributed to a particular individual sensor.</p> <p data-bbox="499 711 753 738">Welch Thesis at 62.</p> <p data-bbox="499 779 1942 1138"><b>The Kalman filter operates in a predictor-corrector fashion, repeating a single time update and measurement update step whenever a new measurement vector becomes available. In the time update step the filter predicts what the state should be at the time of the measurements, based on the previous state estimate and a model of the process dynamics. In the measurement update step the filter uses the newly available measurement vector to correct the predicted state.</b> In a normal implementation, depicted in figure 3.2, the time and measurement steps do not occur until all of the components of the measurement vector are available, i.e. until the state can be determined uniquely from the measurement vector. The measurement update step then processes the entire measurement vector in one batch, e.g. all three measurements in figure 3.2. This batch processing of the measurement data is relatively inflexible and can be computationally expensive if the measurement vector is large.</p> <p data-bbox="499 1146 753 1174">Welch Thesis at 65.</p> <p data-bbox="499 1214 1942 1390">The use of a Kalman filter requires not only a dynamic model as described in section 4.2.1, but also a measurement model. The measurement model is used to predict the ideal noise-free response of each sensor and source pair, given the filter’s current estimate of the target state as in equations (4.2) and (4.3). The prediction is then compared with an actual measurement, and the results are used to generate a correction for the filter’ current estimate of the target state.</p> <p data-bbox="499 1398 753 1425">Welch Thesis at 78.</p>

## Exhibit D-21

CLAIM 1	Welch Thesis
	<p>In light of the device isolation discussion in section 2.5.4 on page 61, the application of the above guidelines in the general case leads to the following heuristic for choosing the SCAAT Kalman filter measurement elements (constraints): During each SCAAT Kalman filter measurement update one should observe a single sensor and source pair only. Thus for the two-camera, four-beacon example, we could have immediately determined that each SCAAT Kalman filter measurement update should incorporate the (u,v) image coordinate of one beacon as seen in one camera. Each such observation could in fact be considered a single geometric constraint: the intersection of a line, the line from the beacon to the principal point of the camera lens, and a plane, the image plane.</p> <p>Welch Thesis at 81.</p>  <p><b>Figure 4.2:</b> Geometric view of state change during time update step. Per the derivatives in the state, the target is predicted to move and reorient since the time of the last filter estimate. Note that the target rotation is maintained incrementally in the state so the state orientation is zero before the time update and non-zero afterwards. The derivative elements of the state have been omitted and the spacial relationship exaggerated for clarity.</p> <p>Welch Thesis at 85.</p>



## Exhibit D-21

CLAIM 1	Welch Thesis
	<div data-bbox="514 243 1186 560"> <p><math>P</math> = error covariance (density) before time update</p> <p><math>P^+</math> = error covariance (density) after time update  <math>= A(\delta t)P(t - \delta t)A^T(\delta t) + Q(\delta t)</math></p> </div> <p><b>Figure 4.3:</b> Geometric view of error covariance change during time update step. The change is shown by a growing probability density for each of <math>x</math>, <math>y</math>, and <math>z</math>. Note that reorientation is possible in general, but not for the dynamic model given in section 4.2.1. To visualize with Euclidean dimensions, the density has been limited to 3D: <math>x</math>, <math>y</math>, and <math>z</math> only. The shape, magnitude, and orientation are illustrative only.</p> <p>Welch Thesis at 85.</p>

## Exhibit D-21

## CLAIM 1

## Welch Thesis

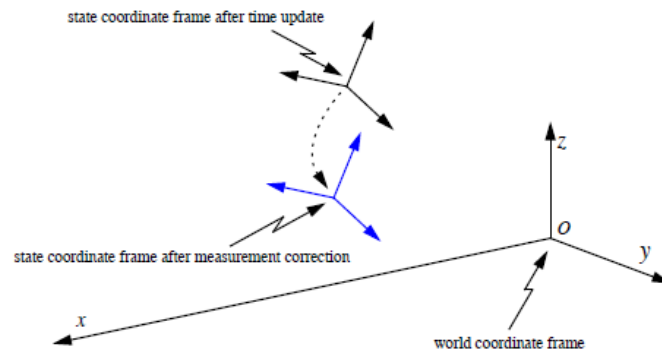


**Figure 4.9:** Geometric view of state change after measurement correction. Per the information in the measurement residual, the *a posteriori* state estimate is formed, i.e. the estimated target coordinate frame is moved and reoriented. Compare this with figure 4.2 on page 85. (Again the derivative elements of the state have been omitted and the spacial relationship exaggerated for clarity.)

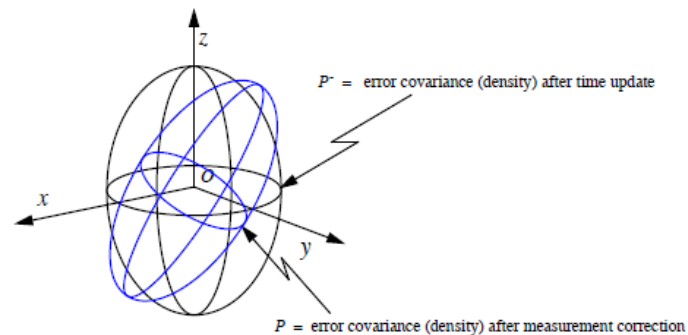


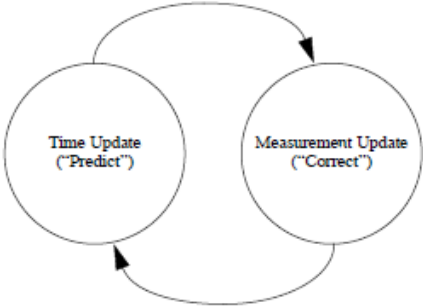
**Figure 4.10:** Geometric view of error covariance change after measurement update. The change is shown by a refined probability density for each of  $x$ ,  $y$ , and  $z$ . Note that in general the density is reoriented to reflect the constraint provided by the measurement. Compare this with figure 4.3 on page 85. (Again to visualize with Euclidean dimensions, the density has been limited to 3D:  $x$ ,  $y$ , and  $z$  only. The absolute shape, magnitude, and orientation are illustrative only.)

Welch Thesis at 95.

## Exhibit D-21

CLAIM 1	Welch Thesis
	<div data-bbox="651 243 1323 649"> </div> <p data-bbox="556 673 1375 763"><b>Figure 4.12:</b> The revised tracking algorithm for autocalibration. The time update consists of equation (4.14). The measurement update consists of equations (4.24)-(4.27), then (4.15)-(4.22), and finally equation (4.28).</p> <p data-bbox="499 787 766 820">Welch Thesis at 102.</p> <p data-bbox="499 852 1963 1177"><b>The Kalman filter estimates a process by using a form of feedback control: the filter estimates the process state at some time and then obtains feedback in the form of (noisy) measurements.</b> As such, the equations for the Kalman filter fall into two groups: time update equations and measurement update equations. The time update equations are responsible for projecting forward (in time) the current state and error covariance estimates to obtain the a priori estimates for the next time step. The measurement update equations are responsible for the feedback—i.e. for incorporating a new measurement into the a priori estimate to obtain an improved a posteriori estimate. The time update equations can also be thought of as predictor equations, while the measurement update equations can be thought of as corrector equations. Indeed the final estimation algorithm resembles that of a predictor-corrector algorithm for solving numerical problems as shown in figure B.1.</p> <p data-bbox="499 1185 808 1218">Welch Thesis at 170-71.</p>

## Exhibit D-21

CLAIM 1	Welch Thesis
	 <p><b>Figure B.1:</b> The ongoing discrete Kalman filter cycle. The <i>time update</i> projects the current state estimate ahead in time. The <i>measurement update</i> adjusts the projected estimate by an actual measurement at that time. Notice the resemblance to a <i>predictor-corrector</i> algorithm</p> <p>Welch Thesis at 171.</p> <p><i>See also</i> Welch Thesis Chapter 2.5 (describing autocalibration for sensor subsystems); Chapter 3.2 (describing sequential estimate updates performed by the SCAAT algorithm as new measurement data is collected by the system); Chapter 4.3 (use of the SCAAT algorithm for tracking to predict and correct sensor measurements); Chapter 4.4 (autocalibration using SCAAT algorithm); Chapter 6.1 (describing autocalibration of HiBall sensor system using SCAAT)</p> <p><i>See also</i> Defendants' Invalidity Contentions for further discussion.</p>

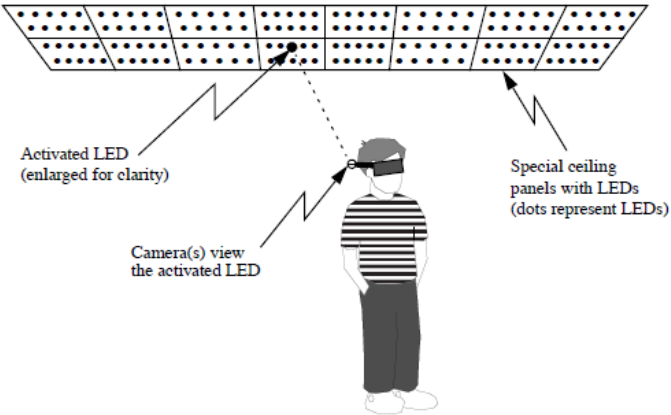
## B. DEPENDENT CLAIM 2

CLAIM 2	Welch Thesis
[2] The method of claim 1 wherein coupling the sensor subsystem to the estimation subsystem	At least under Plaintiffs' apparent infringement theory, Welch Thesis discloses, either expressly or inherently, the method of claim 1 wherein coupling the sensor subsystem to the estimation subsystem includes coupling software modules each associated with one or more of the sensing elements. In the alternative, this element would be

## Exhibit D-21

CLAIM 2	Welch Thesis
includes coupling software modules each associated with one or more of the sensing elements.	<p>obvious over Welch Thesis in light of the other references disclosed in Defendants' Invalidity Contentions and/or the knowledge of one of ordinary skill in the art.</p> <p><i>See, e.g.:</i></p> <p>In this chapter I describe experiments using the SCAAT approach to tracking with the UNC HiBall tracking system. See appendix D for a description of the HiBall tracking system. As part of the development of the HiBall system software, <b>we have built an extensive simulation environment that makes use of detailed mechanical and electrical models that are based on real components.</b> In addition, we have executed the SCAAT computations on the actual target platform to confirm the execution times, etc. See appendix E for a description of the simulation environment. We (Bishop, Chi, Fuchs, Welch et al. at UNC) hope to demonstrate a working HiBall shortly after the publication of this dissertation. Welch Thesis at 119.</p> <p>For the initial implementation of our HiBall system, and thus these simulations, we have decided to implement <b>autocalibration only for the sources, the beacon positions</b>, and not the sensors, the HiBall cameras. Thus the SCAAT implementation is configured to employ both a main HiBall filter as described below in section 6.1.1, and many individual beacon filters—one filter per LED—as described below in section 6.1.2. Welch Thesis at 119.</p> <p>Following the autocalibration method of section 4.4, we <b>maintain a distinct Kalman filter for each individual beacon (LED).</b> Because as described earlier we are primarily concerned with the position of each beacon in world coordinates, this is the per-beacon parameter we have chosen to autocalibrate. Welch Thesis at 120.</p> <p>The tracking system that I employ in my experiments is an “inside-looking-out” optoelectronic system designed for interactive computer graphics or virtual environments. The system, which we call the “HiBall tracker”, is an improved version of the wide-area system described in [Ward92]. <b>In these systems, user-mounted optical sensors observe infrared light-emitting diodes (LEDs) or beacons mounted in the ceiling above the user.</b> The locations of the beacons are known (to some degree) so observations of them can be used to estimate the user's position and orientation. Welch Thesis at 191.</p>

## Exhibit D-21

CLAIM 2	Welch Thesis
	 <p data-bbox="552 662 1218 735"><b>Figure D.1:</b> An outward-looking optoelectronic tracking system. User-mounted cameras look outward (generally upward) at active beacons in the environment.</p> <p data-bbox="514 755 787 787">Welch Thesis at 191.</p> <p data-bbox="514 824 1969 1039">One goal of the HiBall system is to provide a user with <i>wide-area</i> tracking. To this end, the LEDs are installed in special ceiling panels that replace standard-size acoustic ceiling tiles. (See figure D.1.) These tiles can be installed over a large area, thus providing a large working area. In fact, the current UNC installation consists of enough ceiling tiles to cover an area of approximately 5x5 meters, with a corresponding total of over 3,000 LEDs. The LED positions in world coordinates are initially estimated based on the ceiling panel design, which has them installed in a regular two-dimensional grid.</p> <p data-bbox="514 1076 1969 1214">The LEDs are connected to special circuit boards that are mounted on (above) the ceiling tiles, and these circuit boards are then connected to a computer. Thus LEDs can be individually activated under computer control as needed for the SCAAT observations. (The ceiling circuitry allows beacon activation at over 5000 LEDs per second.)</p> <p data-bbox="514 1222 787 1255">Welch Thesis at 192.</p> <p data-bbox="514 1292 1969 1398">In the original system described by [Ward92] the user wore a relatively large head-mounted mechanical fixture that supported several individually self-contained optical sensors or “cameras” and a backpack that contained the necessary signal processing and A/D conversion circuitry as shown in figure D.2.</p>

## Exhibit D-21

CLAIM 2	Welch Thesis
	<p>In the new system the camera fixture and backpack in figure D.2 are together replaced by a relatively small sensor cluster called the HiBall. Figure D.3 is a picture of an unpopulated HiBall with a golf ball to convey a notion of size.</p> <p>A populated HiBall contains six lenses, six photodiodes with infrared filters, and all of the necessary circuitry for signal processing, A/D conversion, control, and high-speed serial communication. <b>It is designed so that each photodiode can view infrared beacons (LEDs in this case) through each of several adjacent lenses, thus implementing up to 26 distinct infrared cameras.</b></p> <p>The photodiodes provide four signals that together indicate the position of the centroid of light (infrared in this case) as it appears on the two-dimensional photodiode surface. <b>At any point in time, the internal A/D conversion circuitry can sample these signals for any one photodiode. These samples would then be sent to an external computer via a high-speed serial link where they would be converted to the measurement that reflect the position of the image of the infrared beacon on the two-dimensional photodiode.</b></p> <p>If the photodiode measurements are viewed as images of the ceiling beacons (known scene points), the HiBall tracker can be viewed as an implementation of the abstract image-based example initially introduced in section 1.2 on page 39 (see figures 1.4-1.6) and later used in chapter 5. Hence my frequent references to a HiBall lens and sensor pair as a camera.</p> <p>Welch Thesis at 192-93.</p> <p><i>See also</i> Defendants' Invalidity Contentions for further discussion.</p>

## C. DEPENDENT CLAIM 5

CLAIM 5	Welch Thesis
[5] The method of claim 1 wherein the state estimate characterizes an	At least under Plaintiffs' apparent infringement theory, Welch Thesis discloses, either expressly or inherently, the method of claim 1 wherein the state estimate characterizes an estimate of a location of the object. In the alternative, this element would be obvious over Welch Thesis in light of the other references disclosed in Defendants' Invalidity Contentions and/or the knowledge of one of ordinary skill in the art.

## Exhibit D-21

CLAIM 5	Welch Thesis
estimate of a location of the object.	<p><i>See, e.g.:</i></p> <p><b>The Kalman filter provides a powerful mathematical framework within which a minimum mean-square-error estimate of a user's position and orientation can be tracked using a sequence of single sensor observations, as opposed to groups of observations.</b> We refer to this new approach as single-constraint-at-a-time or SCAAT tracking. The method improves accuracy by properly assimilating sequential observations, filtering sensor measurements, and by concurrently autocalibrating mechanical or electrical devices. The method facilitates user motion prediction, multisensor data fusion, and in systems where the observations are only available sequentially it provides estimates at a higher rate and with lower latency than a multiple-constraint approach.</p> <p>Welch Thesis at Abstract.</p> <p>If one is uncertain about the <b>3D locations of the beacons</b>, and/or wishes to calibrate (estimate) the positions concurrently while tracking, then guideline (b) would break these two sets into eight sets, each with one 2D camera and one beacon. Finally, per guideline (c) one would note that the eight camera-beacon pairs each yield a (u, v) image coordinate, i.e. <math>ms = 2</math> scalar elements. If there were more source and sensor types, one would repeat this process per guideline (d).</p> <p>Welch Thesis at 80-81.</p> <p>While the total additional floating-point operations presented in table 5.2 may appear daunting, keep in mind that for a SCAAT implementation (in particular) <math>m</math> is likely to be relatively small, e.g. <math>m = 2</math> for the previous image-based examples. In addition, <math>n_\pi</math> is likely to be relatively small for most devices, e.g. <math>n_\pi = n_b = 3</math> when trying to autocalibrate (better estimate) scene point locations for the same example system.</p> <p>Welch Thesis at 115</p> <p>To use Powell's method, I needed to define a cost function that returned a scalar indication of the "goodness" of a particular set of parameters. In simulations I had access to both the estimated filter state and the "true" state (see "Motion Bandwidth" below) for several motion data sets as described in section E.1. Again employing a scheme similar to that of Azuma and Bishop, I designed a special simulation framework for the purpose of parameter optimization. At every filter update step I compute the locations (in world coordinates) of three points arranged in a triangle that is oriented upright and faces the HiBall approximately one meter in front of the HiBall. I compute these three points for both the estimated filter state and the true state, and then I compute the average</p>



## Exhibit D-21

CLAIM 5	Welch Thesis
	<p>distance between the respective estimated and true point groups. This average distance provides a per-estimate scalar cost, which I then average for an entire simulation run (for a particular data set) to obtain the necessary scalar cost for a particular parameter set <math>P[N]</math>. <b>This approach nicely combines position and orientation error into a single cost.</b> The parameters found using this method for various test cases are given in section 6.2.1 of chapter 6.</p> <p>Welch Thesis at 198</p> <p><i>See also</i> Welch Thesis Chapter 2.5 (describing autocalibration for sensor subsystems); Chapter 3.2 (describing sequential estimate updates performed by the SCAAT algorithm as new measurement data is collected by the system); Chapter 4.3 (use of the SCAAT algorithm for tracking to predict and correct sensor measurements); Chapter 4.4 (autocalibration using SCAAT algorithm); Chapter 6.1 (describing autocalibration of HiBall sensor system using SCAAT)</p> <p><i>See</i> Disclosures with respect to Claim 1, <i>supra</i>; <i>see also</i> Defendants' Invalidity Contentions for further discussion.</p>

## D. DEPENDENT CLAIM 6

CLAIM 6	Welch Thesis
<p>[6] The method of claim 1 wherein the state estimate characterizes configuration information for one or more sensing elements fixed to the object.</p>	<p>At least under Plaintiffs' apparent infringement theory, Welch Thesis discloses, either expressly or inherently, the method of claim 1 wherein the state estimate characterizes configuration information for one or more sensing elements fixed to the object. In the alternative, this element would be obvious over Welch Thesis in light of the other references disclosed in Defendants' Invalidity Contentions and/or the knowledge of one of ordinary skill in the art.</p> <p><i>See, e.g.:</i></p>

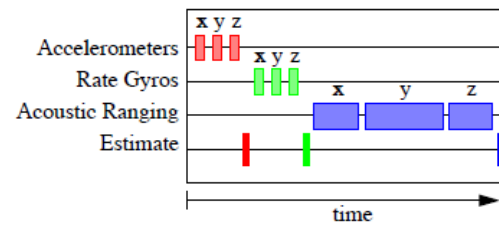
Exhibit D-21

CLAIM 6	Welch Thesis
	<div data-bbox="630 251 1144 706"><p>(a)</p><p>(b)</p><p>(c)</p></div> <p data-bbox="541 722 1176 873"><b>Figure 2.2:</b> State versus parameter estimation. (a) The system parameters are known, and are used with the measurements to estimate the states. (b) For calibration purposes, known states can be used with measurements to estimate the system parameters. (c) A set of parameters can be used in conjunction with measurements to estimate another (not necessarily disjoint) set of parameters <i>and</i> the states.</p> <p data-bbox="514 893 766 933">Welch Thesis at 49.</p> <div data-bbox="609 974 1081 1161"><p>Source Excitation</p><p>Sensor Unit Measurement</p><p>Estimate</p><p>time</p></div> <p data-bbox="529 1177 1213 1258"><b>Figure 2.4:</b> Timing diagram for a (hypothetical) SCAAT magnetic tracker. The state estimate is updated after sensing each individual excitation vector.</p> <p data-bbox="514 1274 766 1315">Welch Thesis at 52.</p>

## Exhibit D-21

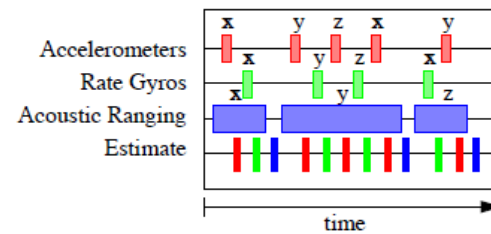
## CLAIM 6

## Welch Thesis



**Figure 2.7:** Timing diagram for a hypothetical conventional hybrid tracking system. The state estimate is updated only after each group of 3 homogeneous measurements.

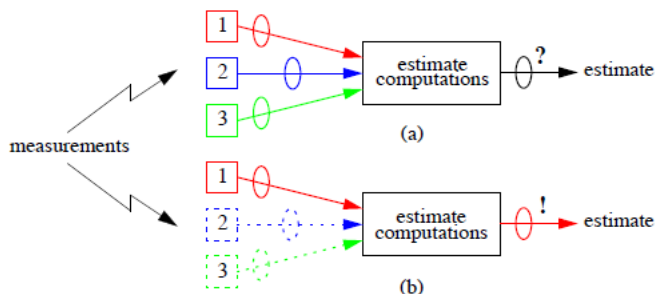
Welch Thesis at 57.



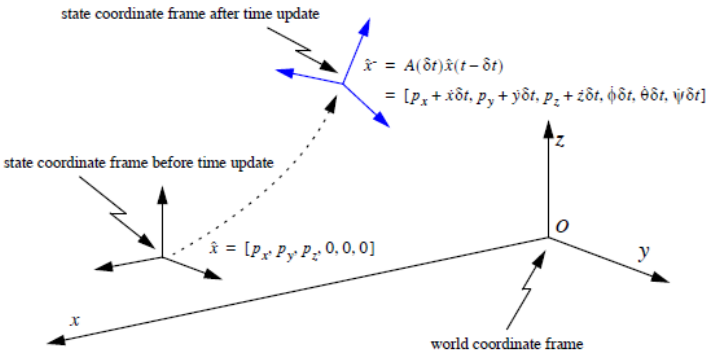
**Figure 2.8:** Timing diagram for a SCAAT inertial-acoustic hybrid tracking system. The state estimate is updated whenever an individual measurement becomes available.

Welch Thesis at 58.

## Exhibit D-21

CLAIM 6	Welch Thesis
	 <p><b>Figure 2.11: Autocalibration and attribution of measurement error.</b> (a) Most algorithms operate on multiple measurements as a group, hence uncertainty or error (represented by the ellipses) in the final estimates is difficult to attribute to any individual sensor. (b) With the SCAAT method, uncertainty in final estimates can more easily be attributed to a particular individual sensor.</p> <p>Welch Thesis at 62.</p> <p>The Kalman filter operates in a predictor-corrector fashion, repeating a single time update and measurement update step whenever a new measurement vector becomes available. In the time update step the filter predicts what the state should be at the time of the measurements, based on the previous state estimate and a model of the process dynamics. In the measurement update step the filter uses the newly available measurement vector to correct the predicted state. In a normal implementation, depicted in figure 3.2, the time and measurement steps do not occur until all of the components of the measurement vector are available, i.e. until the state can be determined uniquely from the measurement vector. The measurement update step then processes the entire measurement vector in one batch, e.g. all three measurements in figure 3.2. This batch processing of the measurement data is relatively inflexible and can be computationally expensive if the measurement vector is large.</p> <p>Welch Thesis at 65.</p> <p>The use of a Kalman filter requires not only a dynamic model as described in section 4.2.1, but also a measurement model. The measurement model is used to predict the ideal noise-free response of each sensor and source pair, given the filter's current estimate of the target state as in equations (4.2) and (4.3). The prediction is then compared with an actual measurement, and the results are used to generate a correction for the filter's current estimate of the target state.</p> <p>Welch Thesis at 78.</p>

## Exhibit D-21

CLAIM 6	Welch Thesis
	<p>In light of the device isolation discussion in section 2.5.4 on page 61, the application of the above guidelines in the general case leads to the following heuristic for choosing the SCAAT Kalman filter measurement elements (constraints): During each SCAAT Kalman filter measurement update one should observe a single sensor and source pair only. Thus for the two-camera, four-beacon example, we could have immediately determined that each SCAAT Kalman filter measurement update should incorporate the (u,v) image coordinate of one beacon as seen in one camera. Each such observation could in fact be considered a single geometric constraint: the intersection of a line, the line from the beacon to the principal point of the camera lens, and a plane, the image plane.</p> <p>Welch Thesis at 81.</p>  <p><b>Figure 4.2:</b> Geometric view of state change during time update step. Per the derivatives in the state, the target is predicted to move and reorient since the time of the last filter estimate. Note that the target rotation is maintained incrementally in the state so the state orientation is zero before the time update and non-zero afterwards. The derivative elements of the state have been omitted and the spacial relationship exaggerated for clarity.</p> <p>Welch Thesis at 85.</p>

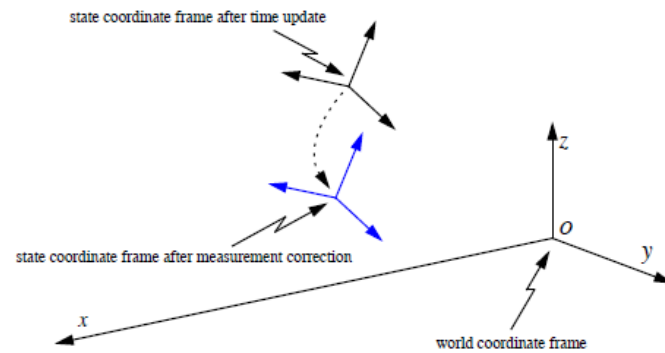
## Exhibit D-21

CLAIM 6	Welch Thesis
	<div data-bbox="529 246 1192 555"> <p> <math>P</math> = error covariance (density) before time update  <math>P^+</math> = error covariance (density) after time update  <math>= A(\delta t)P(t - \delta t)A^T(\delta t) + Q(\delta t)</math> </p> </div> <p> <b>Figure 4.3:</b> Geometric view of error covariance change during time update step. The change is shown by a growing probability density for each of <math>x</math>, <math>y</math>, and <math>z</math>. Note that reorientation is possible in general, but not for the dynamic model given in section 4.2.1. To visualize with Euclidean dimensions, the density has been limited to 3D: <math>x</math>, <math>y</math>, and <math>z</math> only. The shape, magnitude, and orientation are illustrative only.         </p> <p>Welch Thesis at 85.</p>

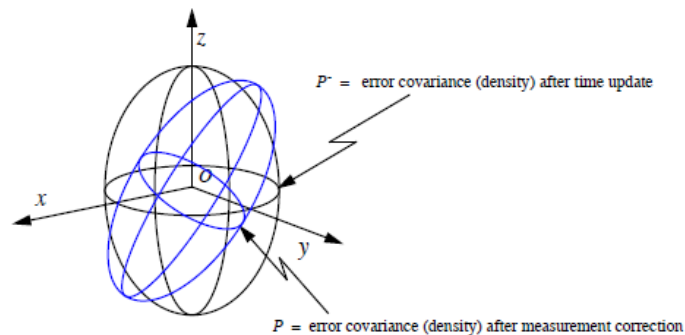
## Exhibit D-21

## CLAIM 6

## Welch Thesis



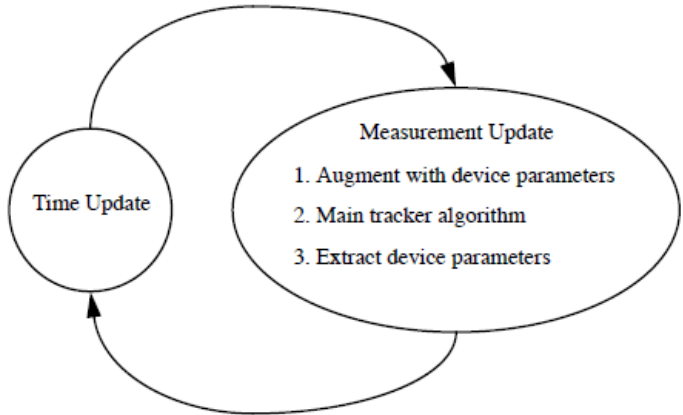
**Figure 4.9:** Geometric view of state change after measurement correction. Per the information in the measurement residual, the *a posteriori* state estimate is formed, i.e. the estimated target coordinate frame is moved and reoriented. Compare this with figure 4.2 on page 85. (Again the derivative elements of the state have been omitted and the spacial relationship exaggerated for clarity.)



**Figure 4.10:** Geometric view of error covariance change after measurement update. The change is shown by a refined probability density for each of  $x$ ,  $y$ , and  $z$ . Note that in general the density is reoriented to reflect the constraint provided by the measurement. Compare this with figure 4.3 on page 85. (Again to visualize with Euclidean dimensions, the density has been limited to 3D:  $x$ ,  $y$ , and  $z$  only. The absolute shape, magnitude, and orientation are illustrative only.)

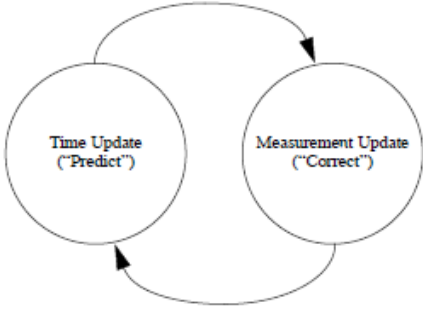
Welch Thesis at 95.

Exhibit D-21

CLAIM 6	Welch Thesis
	<div data-bbox="667 245 1344 657"></div> <p data-bbox="573 672 1383 764"><b>Figure 4.12:</b> The revised tracking algorithm for autocalibration. The time update consists of equation (4.14). The measurement update consists of equations (4.24)-(4.27), then (4.15)-(4.22), and finally equation (4.28).</p> <p data-bbox="514 786 783 816">Welch Thesis at 102.</p> <p data-bbox="514 854 1955 1218"><b>The Kalman filter estimates a process by using a form of feedback control: the filter estimates the process state at some time and then obtains feedback in the form of (noisy) measurements.</b> As such, the equations for the Kalman filter fall into two groups: time update equations and measurement update equations. The time update equations are responsible for projecting forward (in time) the current state and error covariance estimates to obtain the a priori estimates for the next time step. The measurement update equations are responsible for the feedback—i.e. for incorporating a new measurement into the a priori estimate to obtain an improved a posteriori estimate. The time update equations can also be thought of as predictor equations, while the measurement update equations can be thought of as corrector equations. Indeed the final estimation algorithm resembles that of a predictor-corrector algorithm for solving numerical problems as shown in figure B.1. Welch Thesis at 170-71.</p>



## Exhibit D-21

CLAIM 6	Welch Thesis
	 <p><b>Figure B.1:</b> The ongoing discrete Kalman filter cycle. The <i>time update</i> projects the current state estimate ahead in time. The <i>measurement update</i> adjusts the projected estimate by an actual measurement at that time. Notice the resemblance to a <i>predictor-corrector</i> algorithm</p> <p>Welch Thesis at 171.</p> <p>See also Welch Thesis Chapter 2.5 (describing autocalibration for sensor subsystems); Chapter 3.2 (describing sequential estimate updates performed by the SCAAT algorithm as new measurement data is collected by the system); Chapter 4.3 (use of the SCAAT algorithm for tracking to predict and correct sensor measurements); Chapter 4.4 (autocalibration using SCAAT algorithm); Chapter 6.1 (describing autocalibration of HiBall sensor system using SCAAT)</p> <p>See Disclosures with respect to Claim 1, <i>supra</i>; see also Defendants' Invalidity Contentions for further discussion.</p>

## E. DEPENDENT CLAIM 7

CLAIM 7	Welch Thesis
[7] The method of claim 6 wherein the configuration information for the one	At least under Plaintiffs' apparent infringement theory, Welch Thesis discloses, either expressly or inherently, the method of claim 6 wherein the configuration information for the one or more sensing elements fixed to the object includes information related to position or orientation of said sensing elements relative to the object. In the

## Exhibit D-21

CLAIM 7	Welch Thesis
<p>or more sensing elements fixed to the object includes information related to position or orientation of said sensing elements relative to the object.</p>	<p>alternative, this element would be obvious over Welch Thesis in light of the other references disclosed in Defendants' Invalidity Contentions and/or the knowledge of one of ordinary skill in the art.</p> <p><i>See, e.g.:</i></p> <p>The Kalman filter provides a powerful mathematical framework within which a minimum mean-square-error estimate of a user's position and orientation can be tracked using a sequence of single sensor observations, as opposed to groups of observations. We refer to this new approach as single-constraint-at-a-time or SCAAT tracking. The method improves accuracy by properly assimilating sequential observations, filtering sensor measurements, and by concurrently autocalibrating mechanical or electrical devices. The method facilitates user motion prediction, multisensor data fusion, and in systems where the observations are only available sequentially it provides estimates at a higher rate and with lower latency than a multiple-constraint approach.</p> <p>Welch Thesis at Abstract.</p> <div data-bbox="512 732 1178 1200"> <pre> graph LR     subgraph (a)         P1[parameters] --&gt; KF1[Kalman filter]         M1[measurements] --&gt; KF1         KF1 --&gt; SE1[state estimates]     end     subgraph (b)         S1[states] --&gt; KF2[Kalman filter]         M2[measurements] --&gt; KF2         KF2 --&gt; PE2[parameter estimates]     end     subgraph (c)         P2[parameters] --&gt; KF3[Kalman filter]         M3[measurements] --&gt; KF3         KF3 --&gt; PE3[parameter estimates]         KF3 --&gt; SE3[state estimates]     end           </pre> </div> <p><b>Figure 2.2: State versus parameter estimation.</b> (a) The system parameters are known, and are used with the measurements to estimate the states. (b) For calibration purposes, known states can be used with measurements to estimate the system parameters. (c) A set of parameters can be used in conjunction with measurements to estimate another (not necessarily disjoint) set of parameters <i>and</i> the states.</p> <p>Welch Thesis at 49.</p>

## Exhibit D-21

## CLAIM 7

## Welch Thesis

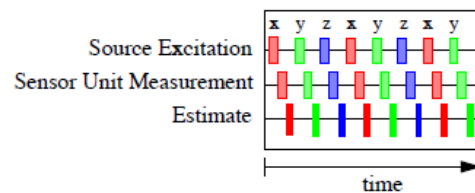


**Figure 2.4:** Timing diagram for a (hypothetical) SCAAT magnetic tracker. The state estimate is updated after sensing each individual excitation vector.

Welch Thesis at 52.

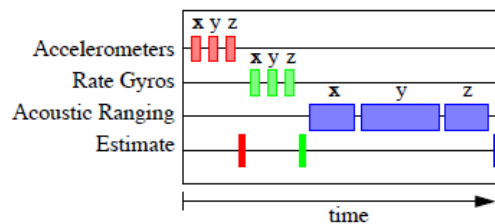


**Figure 2.7:** Timing diagram for a hypothetical conventional hybrid tracking system. The state estimate is updated only after each group of 3 homogeneous measurements.

Welch Thesis at 57.

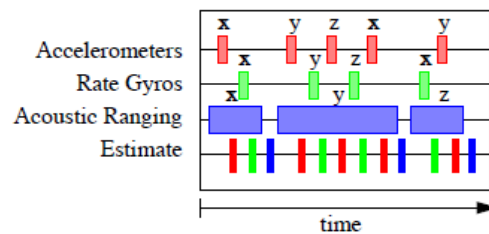


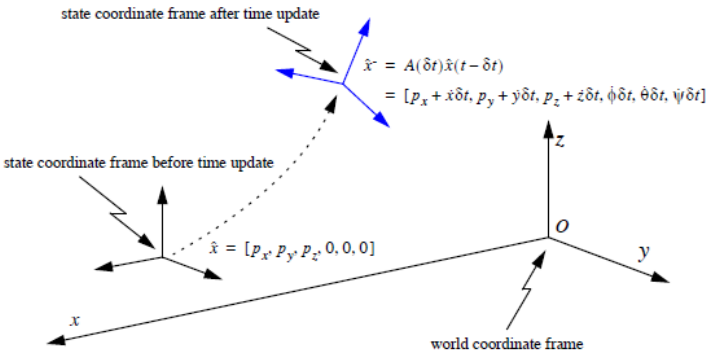
**Figure 2.8:** Timing diagram for a SCAAT inertial-acoustic hybrid tracking system. The state estimate is updated whenever an individual measurement becomes available.

Welch Thesis at 58.

## Exhibit D-21

CLAIM 7	Welch Thesis
	<div data-bbox="514 235 1213 706"> <p>Figure 2.11: Autocalibration and attribution of measurement error. (a) Most algorithms operate on multiple measurements as a group, hence uncertainty or error (represented by the ellipses) in the final estimates is difficult to attribute to any individual sensor. (b) With the SCAAT method, uncertainty in final estimates can more easily be attributed to a particular individual sensor.</p> </div> <p>Welch Thesis at 62.</p> <p>The Kalman filter operates in a predictor-corrector fashion, repeating a single time update and measurement update step whenever a new measurement vector becomes available. In the time update step the filter predicts what the state should be at the time of the measurements, based on the previous state estimate and a model of the process dynamics. In the measurement update step the filter uses the newly available measurement vector to correct the predicted state. In a normal implementation, depicted in figure 3.2, the time and measurement steps do not occur until all of the components of the measurement vector are available, i.e. until the state can be determined uniquely from the measurement vector. The measurement update step then processes the entire measurement vector in one batch, e.g. all three measurements in figure 3.2. This batch processing of the measurement data is relatively inflexible and can be computationally expensive if the measurement vector is large.</p> <p>Welch Thesis at 65.</p> <p>The use of a Kalman filter requires not only a dynamic model as described in section 4.2.1, but also a measurement model. The measurement model is used to predict the ideal noise-free response of each sensor and source pair, given the filter's current estimate of the target state as in equations (4.2) and (4.3). The prediction is then compared with an actual measurement, and the results are used to generate a correction for the filter's current estimate of the target state.</p> <p>Welch Thesis at 78.</p>

## Exhibit D-21

CLAIM 7	Welch Thesis
	<p>In light of the device isolation discussion in section 2.5.4 on page 61, the application of the above guidelines in the general case leads to the following heuristic for choosing the SCAAT Kalman filter measurement elements (constraints): During each SCAAT Kalman filter measurement update one should observe a single sensor and source pair only. Thus for the two-camera, four-beacon example, we could have immediately determined that each SCAAT Kalman filter measurement update should incorporate the (u,v) image coordinate of one beacon as seen in one camera. Each such observation could in fact be considered a single geometric constraint: the intersection of a line, the line from the beacon to the principal point of the camera lens, and a plane, the image plane.</p> <p>Welch Thesis at 81.</p>  <p><b>Figure 4.2:</b> Geometric view of state change during time update step. Per the derivatives in the state, the target is predicted to move and reorient since the time of the last filter estimate. Note that the target rotation is maintained incrementally in the state so the state orientation is zero before the time update and non-zero afterwards. The derivative elements of the state have been omitted and the spacial relationship exaggerated for clarity.</p> <p>Welch Thesis at 85.</p>

## Exhibit D-21

CLAIM 7	Welch Thesis
	<div data-bbox="529 246 1192 555" data-label="Figure"> <p> <math>P</math> = error covariance (density) before time update  <math>P^+</math> = error covariance (density) after time update  <math>= A(\delta t)P(t - \delta t)A^T(\delta t) + Q(\delta t)</math> </p> </div> <p data-bbox="529 571 1192 711"> <b>Figure 4.3:</b> Geometric view of error covariance change during time update step. The change is shown by a growing probability density for each of <math>x</math>, <math>y</math>, and <math>z</math>. Note that reorientation is possible in general, but not for the dynamic model given in section 4.2.1. To visualize with Euclidean dimensions, the density has been limited to 3D: <math>x</math>, <math>y</math>, and <math>z</math> only. The shape, magnitude, and orientation are illustrative only.         </p> <p data-bbox="529 727 1192 760">Welch Thesis at 85.</p>

## Exhibit D-21

CLAIM 7	Welch Thesis
	<div data-bbox="520 261 1178 609"> </div> <p data-bbox="575 621 1178 764"><b>Figure 4.9:</b> Geometric view of state change after measurement correction. Per the information in the measurement residual, the <i>a posteriori</i> state estimate is formed, i.e. the estimated target coordinate frame is moved and reoriented. Compare this with figure 4.2 on page 85. (Again the derivative elements of the state have been omitted and the spacial relationship exaggerated for clarity.)</p> <div data-bbox="541 792 1218 1117"> </div> <p data-bbox="575 1133 1178 1295"><b>Figure 4.10:</b> Geometric view of error covariance change after measurement update. The change is shown by a refined probability density for each of <math>x</math>, <math>y</math>, and <math>z</math>. Note that in general the density is reoriented to reflect the constraint provided by the measurement. Compare this with figure 4.3 on page 85. (Again to visualize with Euclidean dimensions, the density has been limited to 3D: <math>x</math>, <math>y</math>, and <math>z</math> only. The absolute shape, magnitude, and orientation are illustrative only.)</p> <p data-bbox="514 1312 768 1344">Welch Thesis at 95.</p>

Exhibit D-21

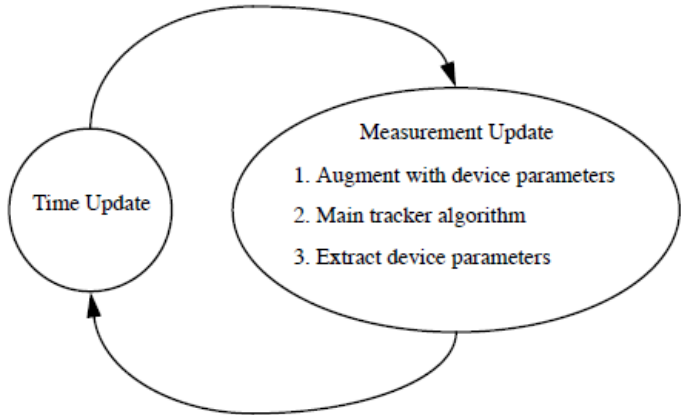
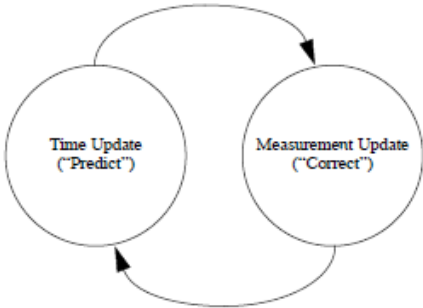
CLAIM 7	Welch Thesis
	<div data-bbox="667 245 1344 657"></div> <p data-bbox="573 672 1383 764"><b>Figure 4.12:</b> The revised tracking algorithm for autocalibration. The time update consists of equation (4.14). The measurement update consists of equations (4.24)-(4.27), then (4.15)-(4.22), and finally equation (4.28).</p> <p data-bbox="514 786 783 816">Welch Thesis at 102.</p> <p data-bbox="514 854 1955 1182"><b>The Kalman filter estimates a process by using a form of feedback control: the filter estimates the process state at some time and then obtains feedback in the form of (noisy) measurements.</b> As such, the equations for the Kalman filter fall into two groups: time update equations and measurement update equations. The time update equations are responsible for projecting forward (in time) the current state and error covariance estimates to obtain the a priori estimates for the next time step. The measurement update equations are responsible for the feedback—i.e. for incorporating a new measurement into the a priori estimate to obtain an improved a posteriori estimate. The time update equations can also be thought of as predictor equations, while the measurement update equations can be thought of as corrector equations. Indeed the final estimation algorithm resembles that of a predictor-corrector algorithm for solving numerical problems as shown in figure B.1.</p> <p data-bbox="514 1187 827 1218">Welch Thesis at 170-71.</p>



Exhibit D-21

CLAIM 7	Welch Thesis
	<div data-bbox="743 248 1163 553"><pre>graph LR; A((Time Update ("Predict"))) --&gt; B((Measurement Update ("Correct"))); B --&gt; A;</pre></div> <p data-bbox="562 605 1360 727"><b>Figure B.1:</b> The ongoing discrete Kalman filter cycle. The <i>time update</i> projects the current state estimate ahead in time. The <i>measurement update</i> adjusts the projected estimate by an actual measurement at that time. Notice the resemblance to a <i>predictor-corrector</i> algorithm</p> <p data-bbox="514 740 785 773">Welch Thesis at 171.</p> <p data-bbox="514 810 1963 1243">To use Powell’s method, I needed to define a cost function that returned a scalar indication of the “goodness” of a particular set of parameters. In simulations I had access to both the estimated filter state and the “true” state (see “Motion Bandwidth” below) for several motion data sets as described in section E.1. Again employing a scheme similar to that of Azuma and Bishop, I designed a special simulation framework for the purpose of parameter optimization. <b>At every filter update step I compute the locations (in world coordinates) of three points arranged in a triangle that is oriented upright and faces the HiBall approximately one meter in front of the HiBall. I compute these three points for both the estimated filter state and the true state, and then I compute the average distance between the respective estimated and true point groups.</b> This average distance provides a per-estimate scalar cost, which I then average for an entire simulation run (for a particular data set) to obtain the necessary scalar cost for a particular parameter set P[N]. This approach nicely combines position and orientation error into a single cost. The parameters found using this method for various test cases are given in section 6.2.1 of chapter 6.</p> <p data-bbox="514 1248 777 1281">Welch Thesis at 198</p> <p data-bbox="514 1318 1963 1422"><i>See also</i> Welch Thesis Chapter 2.5 (describing autocalibration for sensor subsystems); Chapter 3.2 (describing sequential estimate updates performed by the SCAAT algorithm as new measurement data is collected by the system); Chapter 4.3 (use of the SCAAT algorithm for tracking to predict and correct sensor measurements);</p>

## Exhibit D-21

CLAIM 7	Welch Thesis
	<p>Chapter 4.4 (autocalibration using SCAAT algorithm); Chapter 6.1 (describing autocalibration of HiBall sensor system using SCAAT)</p> <p><i>See also</i> Defendants' Invalidity Contentions for further discussion.</p>

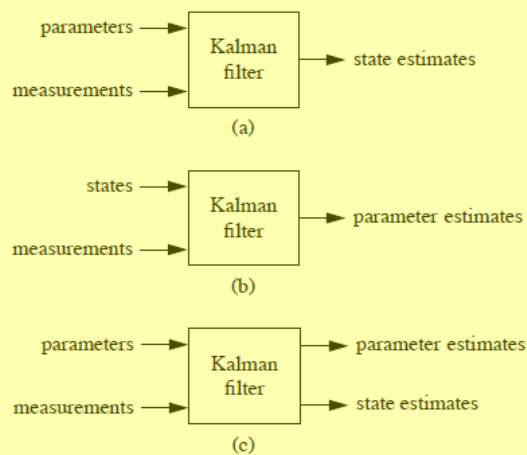
**F. DEPENDENT CLAIM 8**

CLAIM 8	Welch Thesis
<p>[8] The method of claim 6 wherein the configuration information for the one or more sensing elements fixed to the object includes operational parameters for the one or more sensing elements.</p>	<p>At least under Plaintiffs' apparent infringement theory, Welch Thesis discloses, either expressly or inherently, the method of claim 6 wherein the configuration information for the one or more sensing elements fixed to the object includes operational parameters for the one or more sensing elements. In the alternative, this element would be obvious over Welch Thesis in light of the other references disclosed in Defendants' Invalidity Contentions and/or the knowledge of one of ordinary skill in the art.</p> <p><i>See, e.g.:</i></p>

## Exhibit D-21

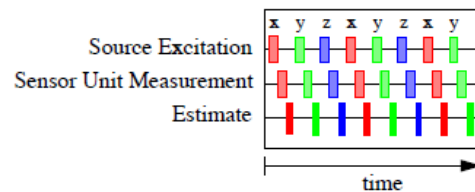
## CLAIM 8

## Welch Thesis



**Figure 2.2:** State versus parameter estimation. (a) The system parameters are known, and are used with the measurements to estimate the states. (b) For calibration purposes, known states can be used with measurements to estimate the system parameters. (c) A set of parameters can be used in conjunction with measurements to estimate another (not necessarily disjoint) set of parameters *and* the states.

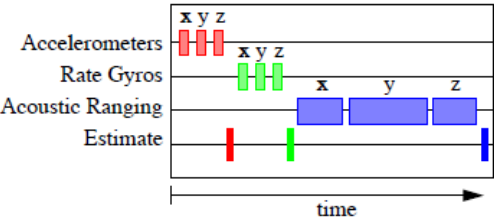
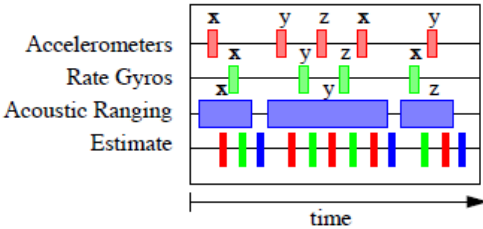
Welch Thesis at 49.



**Figure 2.4:** Timing diagram for a (hypothetical) SCAAT magnetic tracker. The state estimate is updated after sensing each individual excitation vector.

Welch Thesis at 52.

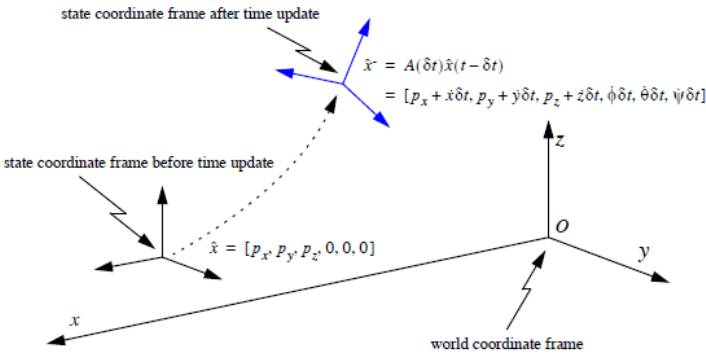
Exhibit D-21

CLAIM 8	Welch Thesis
	<div data-bbox="625 248 1115 467"></div> <div data-bbox="541 480 1218 557"><p><b>Figure 2.7:</b> Timing diagram for a hypothetical conventional hybrid tracking system. The state estimate is updated only after each group of 3 homogeneous measurements.</p></div> <p data-bbox="516 570 768 602">Welch Thesis at 57.</p> <div data-bbox="667 646 1146 873"></div> <div data-bbox="562 886 1266 967"><p><b>Figure 2.8:</b> Timing diagram for a SCAAT inertial-acoustic hybrid tracking system. The state estimate is updated whenever an individual measurement becomes available.</p></div> <p data-bbox="516 997 768 1029">Welch Thesis at 58.</p>

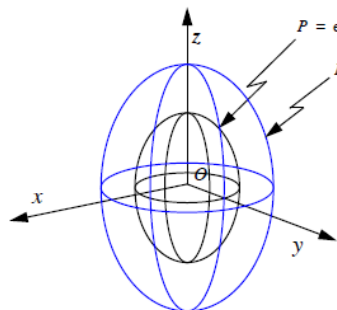
## Exhibit D-21

CLAIM 8	Welch Thesis
	<div data-bbox="514 235 1213 706"> <p>Figure 2.11: Autocalibration and attribution of measurement error. (a) Most algorithms operate on multiple measurements as a group, hence uncertainty or error (represented by the ellipses) in the final estimates is difficult to attribute to any individual sensor. (b) With the SCAAT method, uncertainty in final estimates can more easily be attributed to a particular individual sensor.</p> </div> <p>Welch Thesis at 62.</p> <p>The Kalman filter operates in a predictor-corrector fashion, repeating a single time update and measurement update step whenever a new measurement vector becomes available. In the time update step the filter predicts what the state should be at the time of the measurements, based on the previous state estimate and a model of the process dynamics. In the measurement update step the filter uses the newly available measurement vector to correct the predicted state. In a normal implementation, depicted in figure 3.2, the time and measurement steps do not occur until all of the components of the measurement vector are available, i.e. until the state can be determined uniquely from the measurement vector. The measurement update step then processes the entire measurement vector in one batch, e.g. all three measurements in figure 3.2. This batch processing of the measurement data is relatively inflexible and can be computationally expensive if the measurement vector is large.</p> <p>Welch Thesis at 65.</p> <p>The use of a Kalman filter requires not only a dynamic model as described in section 4.2.1, but also a measurement model. The measurement model is used to predict the ideal noise-free response of each sensor and source pair, given the filter's current estimate of the target state as in equations (4.2) and (4.3). The prediction is then compared with an actual measurement, and the results are used to generate a correction for the filter's current estimate of the target state.</p> <p>Welch Thesis at 78.</p>

## Exhibit D-21

CLAIM 8	Welch Thesis
	<p>In light of the device isolation discussion in section 2.5.4 on page 61, the application of the above guidelines in the general case leads to the following heuristic for choosing the SCAAT Kalman filter measurement elements (constraints): During each SCAAT Kalman filter measurement update one should observe a single sensor and source pair only. Thus for the two-camera, four-beacon example, we could have immediately determined that each SCAAT Kalman filter measurement update should incorporate the (u,v) image coordinate of one beacon as seen in one camera. Each such observation could in fact be considered a single geometric constraint: the intersection of a line, the line from the beacon to the principal point of the camera lens, and a plane, the image plane.</p> <p>Welch Thesis at 81.</p>  <p><b>Figure 4.2:</b> Geometric view of state change during time update step. Per the derivatives in the state, the target is predicted to move and reorient since the time of the last filter estimate. Note that the target rotation is maintained incrementally in the state so the state orientation is zero before the time update and non-zero afterwards. The derivative elements of the state have been omitted and the spacial relationship exaggerated for clarity.</p> <p>Welch Thesis at 85.</p>

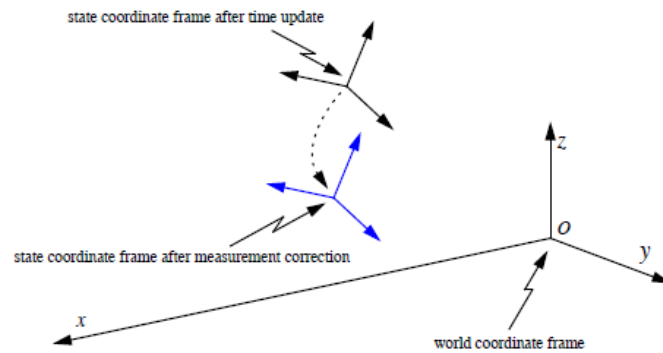
## Exhibit D-21

CLAIM 8	Welch Thesis
	<div data-bbox="527 245 1192 553">  <p> <math>P</math> = error covariance (density) before time update  <math>P^+</math> = error covariance (density) after time update  <math>= A(\delta t)P(t - \delta t)A^T(\delta t) + Q(\delta t)</math> </p> </div> <p data-bbox="527 570 1192 708"><b>Figure 4.3:</b> Geometric view of error covariance change during time update step. The change is shown by a growing probability density for each of <math>x</math>, <math>y</math>, and <math>z</math>. Note that reorientation is possible in general, but not for the dynamic model given in section 4.2.1. To visualize with Euclidean dimensions, the density has been limited to 3D: <math>x</math>, <math>y</math>, and <math>z</math> only. The shape, magnitude, and orientation are illustrative only.</p> <p data-bbox="527 727 768 760">Welch Thesis at 85.</p>

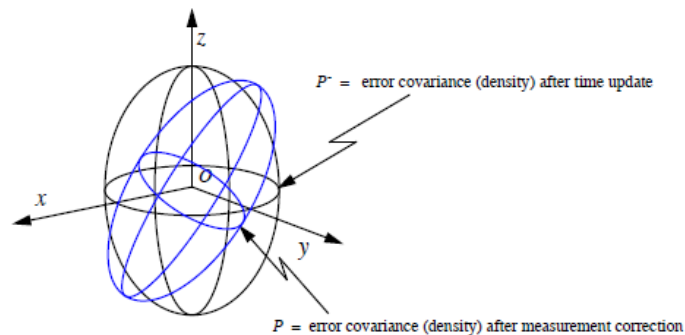
## Exhibit D-21

## CLAIM 8

## Welch Thesis



**Figure 4.9:** Geometric view of state change after measurement correction. Per the information in the measurement residual, the *a posteriori* state estimate is formed, i.e. the estimated target coordinate frame is moved and reoriented. Compare this with figure 4.2 on page 85. (Again the derivative elements of the state have been omitted and the spacial relationship exaggerated for clarity.)

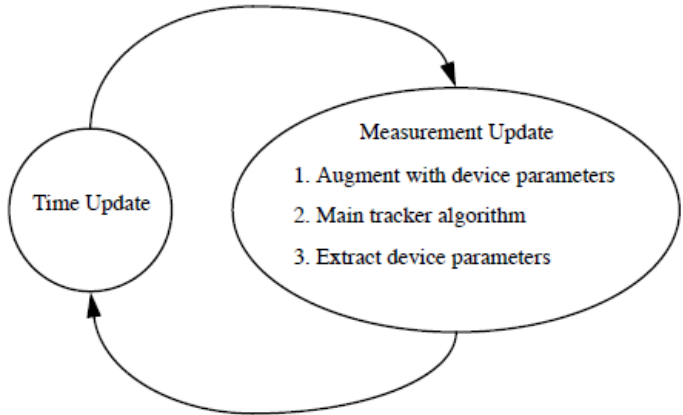


**Figure 4.10:** Geometric view of error covariance change after measurement update. The change is shown by a refined probability density for each of  $x$ ,  $y$ , and  $z$ . Note that in general the density is reoriented to reflect the constraint provided by the measurement. Compare this with figure 4.3 on page 85. (Again to visualize with Euclidean dimensions, the density has been limited to 3D:  $x$ ,  $y$ , and  $z$  only. The absolute shape, magnitude, and orientation are illustrative only.)

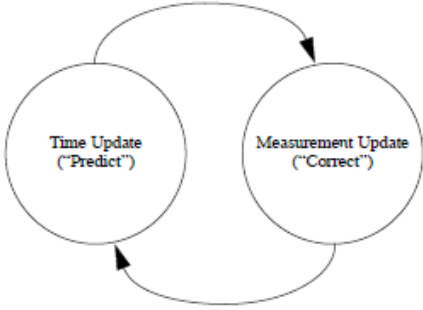
Welch Thesis at 95.



Exhibit D-21

CLAIM 8	Welch Thesis
	<div data-bbox="667 245 1344 657"></div> <p data-bbox="573 672 1383 764"><b>Figure 4.12:</b> The revised tracking algorithm for autocalibration. The time update consists of equation (4.14). The measurement update consists of equations (4.24)-(4.27), then (4.15)-(4.22), and finally equation (4.28).</p> <p data-bbox="514 786 783 816">Welch Thesis at 102.</p> <p data-bbox="514 854 1963 1182">The Kalman filter estimates a process by using a form of feedback control: the filter estimates the process state at some time and then obtains feedback in the form of (noisy) measurements. As such, the equations for the Kalman filter fall into two groups: time update equations and measurement update equations. The time update equations are responsible for projecting forward (in time) the current state and error covariance estimates to obtain the a priori estimates for the next time step. The measurement update equations are responsible for the feedback—i.e. for incorporating a new measurement into the a priori estimate to obtain an improved a posteriori estimate. The time update equations can also be thought of as predictor equations, while the measurement update equations can be thought of as corrector equations. Indeed the final estimation algorithm resembles that of a predictor-corrector algorithm for solving numerical problems as shown in figure B.1.</p> <p data-bbox="514 1187 825 1218">Welch Thesis at 170-71.</p>

## Exhibit D-21

CLAIM 8	Welch Thesis
	 <p><b>Figure B.1:</b> The ongoing discrete Kalman filter cycle. The <i>time update</i> projects the current state estimate ahead in time. The <i>measurement update</i> adjusts the projected estimate by an actual measurement at that time. Notice the resemblance to a <i>predictor-corrector</i> algorithm</p> <p>Welch Thesis at 171.</p> <p><i>See also</i> Welch Thesis Chapter 2.5 (describing autocalibration for sensor subsystems); Chapter 3.2 (describing sequential estimate updates performed by the SCAAT algorithm as new measurement data is collected by the system); Chapter 4.3 (use of the SCAAT algorithm for tracking to predict and correct sensor measurements); Chapter 4.4 (autocalibration using SCAAT algorithm); Chapter 6.1 (describing autocalibration of HiBall sensor system using SCAAT)</p> <p><i>See also</i> Defendants' Invalidity Contentions for further discussion.</p>

## G. DEPENDENT CLAIM 24

CLAIM 24	Welch Thesis
[24] The method of claim 1 wherein updating the state estimate	At least under Plaintiffs' apparent infringement theory, Welch Thesis discloses, either expressly or inherently, the method of claim 1 wherein updating the state estimate includes applying a Kalman Filter approach. In the alternative, this element would be obvious over Welch Thesis in light of the other references disclosed in Defendants' Invalidity Contentions and/or the knowledge of one of ordinary skill in the art.

## Exhibit D-21

CLAIM 24	Welch Thesis
includes applying a Kalman Filter approach.	<p><i>See, e.g.:</i></p> <p><b>The Kalman filter provides a powerful mathematical framework</b> within which a minimum mean-square-error estimate of a user's position and orientation can be tracked using a sequence of <i>single</i> sensor observations, as opposed to <i>groups</i> of observations. <b>We refer to this new approach as single-constraint-at-a-time or SCAAT tracking.</b> The method improves accuracy by properly assimilating sequential observations, filtering sensor measurements, and by concurrently <i>autocalibrating</i> mechanical or electrical devices. The method facilitates user motion prediction, multisensor data fusion, and in systems where the observations are only available sequentially it provides estimates at a higher rate and with lower latency than a multiple-constraint approach.</p> <p>Improved accuracy is realized primarily for three reasons. First, the method avoids mathematically treating truly sequential observations as if they were simultaneous. Second, because each estimate is based on the observation of an individual device, perceived error (statistically unusual estimates) can be more directly attributed to the corresponding device. This can be used for concurrent autocalibration which can be elegantly incorporated into the existing Kalman filter. Third, the Kalman filter inherently addresses the effects of noisy device measurements. Beyond accuracy, the method nicely facilitates motion prediction because the Kalman filter already incorporates a model of the user's dynamics, and because it provides smoothed estimates of the user state, including potentially unmeasured elements. Finally, in systems where the observations are only available sequentially, the method can be used to weave together information from individual devices in a very flexible manner, producing a new estimate as soon as each individual observation becomes available, thus facilitating multisensor data fusion and improving the estimate rates and latencies.</p> <p>Welch Thesis at Abstract.</p> <p><b>A Kalman filter can be used to estimate a globally-observable process by sequentially incorporating only measurements of locally-unobservable processes.</b> The use of a Kalman filter in such a manner offers several advantages: (1) a flexible framework for heterogeneous multisensor data fusion; (2) a unique opportunity to perform concurrent device autocalibration; and in a system that allows only sequential measurements, (3) significantly improved estimate rates and latencies; and (4) avoidance of the incorrect simultaneity assumption.</p> <p>Welch Thesis at 43.</p> <p><b>There are four typical reasons why people employ Kalman filters in systems where a signal (often continuous) is to be estimated with a sequence of discrete measurements or observations: (1) filtering; (2) data fusion; (3) prediction; and (4) calibration.</b></p> <p>Welch Thesis at 44.</p>

## Exhibit D-21

CLAIM 24	Welch Thesis
	<p>The Kalman filter is a set of mathematical equations that provides an efficient computational (recursive) means of using noisy measurements to estimate the state of a linear system, while minimizing the expected mean-squared estimation error. Welch Thesis at 45.</p> <p><b>The Kalman filter is generally presented as a way of estimating values of stochastic variables (the states) of linear systems whose associated system parameters (e.g. model dynamics and noise characteristics) have known values.</b> Interestingly enough, the filter can just as well be turned around and used to estimate values of unknown system parameters when the states are known [Jacobs93]. In fact, it can even be used to estimate both system states and parameters as represented in figure 2.2.</p> <p>In particular, the characteristics outlined in sections 2.1.1 and 2.1.2 make the Kalman filter an attractive and popular option for calibration. Referring to figure 2.2, the situation depicted in (a) is that of a Kalman filter being used only to estimate the system states, i.e. there is no calibration. Examples of the situation depicted in (b) include [Wefald84] and [Foxlin96]. Recent examples of the situation depicted in (c) include [Azarbayejani95] and the work presented in this dissertation. Welch Thesis at 48.</p>

Exhibit D-21

CLAIM 24	Welch Thesis
	<div><p>Figure 2.2 consists of three sub-diagrams, (a), (b), and (c), each showing a 'Kalman filter' block. In (a), 'parameters' and 'measurements' are inputs, and 'state estimates' is the output. In (b), 'states' and 'measurements' are inputs, and 'parameter estimates' is the output. In (c), 'parameters' and 'measurements' are inputs, and both 'parameter estimates' and 'state estimates' are outputs. The three diagrams are arranged vertically and are highlighted by a yellow background.</p><p><b>Figure 2.2:</b> State versus parameter estimation. (a) The system parameters are known, and are used with the measurements to estimate the states. (b) For calibration purposes, known states can be used with measurements to estimate the system parameters. (c) A set of parameters can be used in conjunction with measurements to estimate another (not necessarily disjoint) set of parameters <i>and</i> the states.</p><p>Welch Thesis at 49.</p><p>Given a set of unknowns, and a set of equations (linear or nonlinear) that simultaneously describe a known relationship between the unknowns, several methods exist for solving for the unknowns. For several examples, see [Press90]. <b>The Kalman filter can also be used to estimate the unknowns by mapping the given equations and constraints into the Kalman filter framework.</b> Furthermore, I believe that it would be interesting to investigate the application of the SCAAT method to this problem.</p><p>Welch Thesis at 158</p><p><i>See also</i> Welch Thesis Chapter 4 (describing implementation of Kalman filter in the SCAAT tracking method); Welch Thesis Appendix B (providing a “ready and accessible introduction to both the discrete Kalman filter and the extended Kalman filter”).</p></div>

## Exhibit D-21

CLAIM 24	Welch Thesis
	<i>See also</i> Defendants' Invalidity Contentions for further discussion.

## H. DEPENDENT CLAIM 25

CLAIM 25	Welch Thesis
[25] The method of claim 1 wherein each of said sensing elements comprises at least one of a sensor and a target.	<p>At least under Plaintiffs' apparent infringement theory, Welch Thesis discloses, either expressly or inherently, the method of claim 1 wherein each of said sensing elements comprises at least one of a sensor and a target. In the alternative, this element would be obvious over Welch Thesis in light of the other references disclosed in Defendants' Invalidity Contentions and/or the knowledge of one of ordinary skill in the art.</p> <p><i>See, e.g.:</i></p> <p>Throughout this dissertation I refer to <b>"sources", "sensors", or "devices"</b>, and it's particularly important to understand what I mean by these words not only to avoid confusion, but to understand the basic SCAAT approach. I use the words <b>"source" or "sensor" to refer to the single (minimal) electrical or mechanical component used to excite or sense a particular physical medium.</b> Using this nomenclature, some <b>example sources include a single-axis electromagnetic dipole, an infrared LED, and a single GPS satellite.</b> Some example sensors include a single-axis electromagnetic coil, a single camera, and a GPS receiver. I will use the word <b>"device" to refer to either a source or sensor. On the other hand, when I want to refer to a mechanical fixture that incorporates multiple sources or sensors, I will use phrases such as "source unit" or "sensing unit".</b></p> <p>Welch Thesis at 35</p> <p>The use of a Kalman filter requires not only a dynamic model as described in section 4.2.1, but also a measurement model. <b>The measurement model is used to predict the ideal noise-free response of each sensor and source pair,</b> given the filter's current estimate of the target state as in equations (4.2) and (4.3). The prediction is then compared with an actual measurement, and the results are used to generate a correction for the filter's current estimate of the target state.</p> <p>Welch Thesis at 78.</p>

## Exhibit D-21

CLAIM 25	Welch Thesis
	<p>In choosing the measurement elements to incorporate during a SCAAT Kalman filter measurement update one must consider the available sources and sensors as described in “Defining the Nomenclature” on page 35, and then identify the constraints and corresponding measurements that will be used to update the filter. Recall from “A Single Constraint” on page 37 that in the purest mathematical sense, a single constraint corresponds to one scalar equation describing a known relationship between the unknown state vector elements. Correspondingly a SCAAT Kalman filter should, in the purest sense, generate each new estimate with only a single scalar measurement from one source and sensor pair. Welch Thesis at 79.</p> <p>So given the preceding discussion, what criteria should one use when choosing the measurement elements or constraints to incorporate during a SCAAT Kalman filter measurement update? Given the complete set of available sources and sensors for the system, I suggest the following guidelines:</p> <ol style="list-style-type: none"> <li>begin by <b>identifying the set of all sensor and corresponding source elements</b> that can possibly be observed at any one instant in time;</li> <li>within this set <b>identify any single source and sensor pairs</b> that should be isolated from the others;</li> <li>for each such pair identify the scalar elements yielded from a measurement of the sensor with the corresponding source; and</li> <li>apply these guidelines until all the available sources and sensors have been considered.</li> </ol> <p>Welch Thesis at 80.</p> <p>Consider, for example, tracking <b>two rigidly mounted 2D cameras that can observe four fixed beacons or scene points</b>, as depicted for one camera in figure 1.4 on page 39. The combined use of two sensors (the 2D cameras) and four sources (the beacons) yields a total of 16 scalar measurement elements for the complete set of sources and sensors: a pair for each of four beacons as seen by each of two cameras. If the two cameras cannot be shuttered and scanned-out simultaneously then guideline (a) would reduce the original set to two new sets, each with one 2D camera and four beacons. If one is uncertain about the 3D locations of the beacons, and/or wishes to calibrate (estimate) the positions concurrently while tracking, then guideline (b) would break these two sets into eight sets, each with one 2D camera and one beacon. Finally, per guideline (c) one would note that the eight camera-beacon pairs each yield a image coordinate, i.e. scalar elements. If there were more source and sensor</p>

## Exhibit D-21

CLAIM 25	Welch Thesis
	<p>types, one would repeat this process per guideline (d). Welch Thesis at 80-81.</p> <p>In light of the device isolation discussion in section 2.5.4 on page 61, the application of the above guidelines in the general case leads to the following heuristic for choosing the SCAAT Kalman filter measurement elements (constraints):</p> <p>During each SCAAT Kalman filter measurement update one should observe a single sensor and source pair only.</p> <p>Thus for the two-camera, four-beacon example, we could have immediately determined that each SCAAT Kalman filter measurement update should incorporate the image coordinate of one beacon as seen in one camera. Each such observation could in fact be considered a single geometric constraint: the intersection of a line, the line from the beacon to the principal point of the camera lens, and a plane, the image plane. Welch Thesis at 81.</p> <p>With respect to the SCAAT method, we have chosen to define a single constraint for the HiBall tracking system as <b>one observation of one beacon with one HiBall lens and sensor pair</b>. Thus the measurement vector given in equation (4.10) and the respective components in equations (4.11) and (4.12) are all two-dimensional, i.e. . The situation is similar to that depicted in figure 1.6 on page 41. Welch Thesis at 123.</p> <p>If the photodiode measurements are viewed as images of the ceiling beacons (known scene points), the HiBall tracker can be viewed as an implementation of the abstract image-based example initially introduced in section 1.2 on page 39 (see figures 1.4-1.6) and later used in chapter 5. Hence my frequent references to a HiBall lens and sensor pair as a camera. Welch Thesis at 193</p> <p><i>See Disclosures with respect to Claim 1, supra; see also Defendants' Invalidity Contentions for further discussion.</i></p>

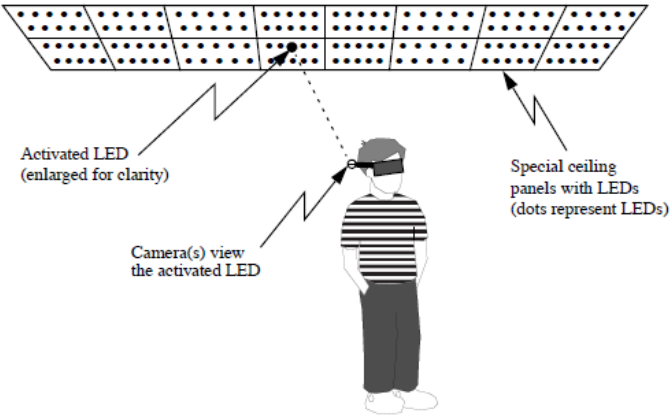


## Exhibit D-21

**I. DEPENDENT CLAIM 28**

CLAIM 28	Welch Thesis
<p>[28] The method of claim 1 wherein the object is selected from a group consisting of a vehicle, a robot, a person, a part of a person, a flying object, a floating object, an underwater moving object, an animal, a camera, a sensing apparatus, a helmet, a tool, a piece of sports equipment, a shoe, a boot, an article of clothing, a personal protective equipment, a rigid object having a dimension between 1 nanometer to 109 meters.</p>	<p>At least under Plaintiffs' apparent infringement theory, Welch Thesis discloses, either expressly or inherently, the method of claim 1 wherein the object is selected from a group consisting of a vehicle, a robot, a person, a part of a person, a flying object, a floating object, an underwater moving object, an animal, a camera, a sensing apparatus, a helmet, a tool, a piece of sports equipment, a shoe, a boot, an article of clothing, a personal protective equipment, a rigid object having a dimension between 1 nanometer to 109 meters. In the alternative, this element would be obvious over Welch Thesis in light of the other references disclosed in Defendants' Invalidity Contentions and/or the knowledge of one of ordinary skill in the art.</p> <p><i>See, e.g.:</i></p> <p>The tracking system that I employ in my experiments is an "inside-looking-out" optoelectronic system designed for interactive computer graphics or virtual environments. The system, which we call the "HiBall tracker", is an improved version of the wide-area system described in [Ward92]. In these systems, user-mounted optical sensors observe infrared light-emitting diodes (LEDs) or beacons mounted in the ceiling above the user. The locations of the beacons are known (to some degree) so observations of them can be used to estimate the user's position and orientation.</p> <p>Welch Thesis at 191.</p>

## Exhibit D-21

CLAIM 28	Welch Thesis
	 <p><b>Figure D.1:</b> An outward-looking optoelectronic tracking system. User-mounted cameras look outward (generally upward) at active beacons in the environment.</p> <p>Welch Thesis at 191.</p> <p>One goal of the HiBall system is to provide a user with <i>wide-area</i> tracking. To this end, the LEDs are installed in special ceiling panels that replace standard-size acoustic ceiling tiles. (See figure D.1.) These tiles can be installed over a large area, thus providing a large working area. In fact, the current UNC installation consists of enough ceiling tiles to cover an area of approximately 5x5 meters, with a corresponding total of over 3,000 LEDs. The LED positions in world coordinates are initially estimated based on the ceiling panel design, which has them installed in a regular two-dimensional grid.</p> <p>The LEDs are connected to special circuit boards that are mounted on (above) the ceiling tiles, and these circuit boards are then connected to a computer. Thus LEDs can be individually activated under computer control as needed for the SCAAT observations. (The ceiling circuitry allows beacon activation at over 5000 LEDs per second.)</p> <p>Welch Thesis at 192.</p> <p>In the original system described by [Ward92] the user wore a relatively large head-mounted mechanical fixture that supported several individually self-contained optical sensors or “cameras” and a backpack that contained the necessary signal processing and A/D conversion circuitry as shown in figure D.2.</p>

## Exhibit D-21

CLAIM 28	Welch Thesis
	<p>In the new system the camera fixture and backpack in figure D.2 are together replaced by a relatively small sensor cluster called the HiBall. Figure D.3 is a picture of an unpopulated HiBall with a <b>golf ball</b> to convey a notion of size.</p> <p>A populated HiBall contains six lenses, six photodiodes with infrared filters, and all of the necessary circuitry for signal processing, A/D conversion, control, and high-speed serial communication. It is designed so that each photodiode can view infrared beacons (LEDs in this case) through each of several adjacent lenses, thus implementing up to 26 distinct infrared cameras.</p> <p>The photodiodes provide four signals that together indicate the position of the centroid of light (infrared in this case) as it appears on the two-dimensional photodiode surface. At any point in time, the internal A/D conversion circuitry can sample these signals for any one photodiode. These samples would then be sent to an external computer via a high-speed serial link where they would be converted to the measurement that reflect the position of the image of the infrared beacon on the two-dimensional photodiode.</p> <p>If the photodiode measurements are viewed as images of the ceiling beacons (known scene points), the HiBall tracker can be viewed as an implementation of the abstract image-based example initially introduced in section 1.2 on page 39 (see figures 1.4-1.6) and later used in chapter 5. Hence my frequent references to a HiBall lens and sensor pair as a camera. Welch Thesis at 192-93.</p> <p><i>See Disclosures with respect to Claim 1, supra; see also Defendants' Invalidity Contentions for further discussion.</i></p>

**J. DEPENDENT CLAIM 29**

CLAIM 29	Welch Thesis
[29] The method of claim 1 wherein the state estimate comprises information related to a position or an orientation	At least under Plaintiffs' apparent infringement theory, Welch Thesis discloses, either expressly or inherently, the method of claim 1 wherein the state estimate comprises information related to a position or an orientation of the object relative to a reference coordinate frame. In the alternative, this element would be obvious over Welch Thesis in light of the other references disclosed in Defendants' Invalidity Contentions and/or the knowledge of one of ordinary skill in the art.

## Exhibit D-21

CLAIM 29	Welch Thesis
of the object relative to a reference coordinate frame.	<p><i>See, e.g.:</i></p> <p><b>2.1.2 Data Fusion</b></p> <p>The Kalman filter assumes that the system being estimated has a <i>measurement equation</i> of the form given in equation (2.1) where the matrix <math>H(t_k)</math> relates the state vector <math>\hat{x}(t_k)</math> to the measurement vector <math>\hat{z}(t_k)</math>, and the vector <math>\hat{v}(t_k)</math> represents the measurement noise. Further details are presented in chapter 4 and can be found in Kalman filter texts such as [Brown92, Gelb74, Jacobs93, Lewis86].</p> $\hat{z}(t_k) = H(t_k)\hat{x}(t_k) + \hat{v}(t_k) \quad (2.1)$ <p>If the system being estimated has multiple forms of observation, there would be multiple corresponding measurement equations equation (2.1), i.e. multiple instances of the matrix <math>H(t_k)</math>, each representing a different relationship. By using the appropriate <math>H(t_k)</math> for each type of measurement, the filter effectively combines, blends, or <i>fuses</i> the information contained in the heterogeneous measurements.</p> <p>This capability for heterogeneous <i>data fusion</i>, combined with the properties discussed in section 2.1.1, has made the Kalman filter a very popular means of data fusion. For example the Kalman filter has been used for navigation [Geier87, Mahmoud94, Watanabe94], for virtual environment tracking [Azuma95, Emura94, Foxlin96], and for 3D scene modeling [Grandjean89, VanPabst95].</p> <p>Welch Thesis at 46.</p>

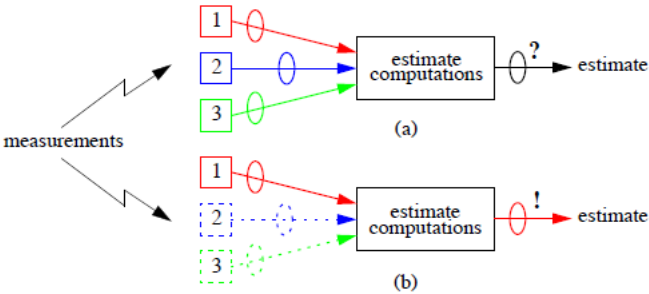
## Exhibit D-21

CLAIM 29	Welch Thesis
	<div data-bbox="625 251 1144 706"> <p>(a)</p> <p>(b)</p> <p>(c)</p> </div> <p><b>Figure 2.2:</b> State versus parameter estimation. (a) The system parameters are known, and are used with the measurements to estimate the states. (b) For calibration purposes, known states can be used with measurements to estimate the system parameters. (c) A set of parameters can be used in conjunction with measurements to estimate another (not necessarily disjoint) set of parameters <i>and</i> the states.</p> <p>Welch Thesis at 49.</p> <div data-bbox="604 974 1081 1161"> </div> <p><b>Figure 2.4:</b> Timing diagram for a (hypothetical) SCAAT magnetic tracker. The state estimate is updated after sensing each individual excitation vector.</p> <p>Welch Thesis at 52.</p>

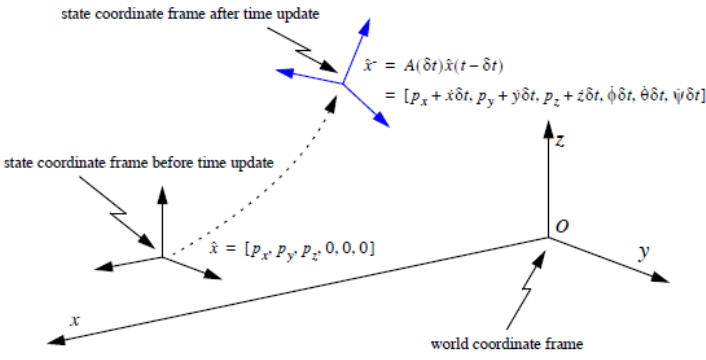
Exhibit D-21

CLAIM 29	Welch Thesis
	<div><p><b>Figure 2.7:</b> Timing diagram for a hypothetical conventional hybrid tracking system. The state estimate is updated only after each group of 3 homogeneous measurements.</p><p>Welch Thesis at 57.</p><p><b>Figure 2.8:</b> Timing diagram for a SCAAT inertial-acoustic hybrid tracking system. The state estimate is updated whenever an individual measurement becomes available.</p><p>Welch Thesis at 58.</p></div>

## Exhibit D-21

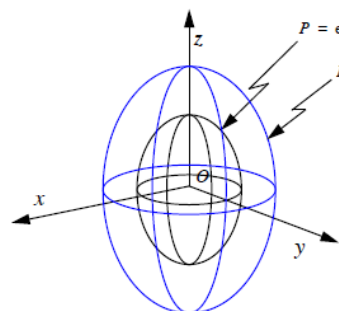
CLAIM 29	Welch Thesis
	 <p><b>Figure 2.11: Autocalibration and attribution of measurement error.</b> (a) Most algorithms operate on multiple measurements as a group, hence uncertainty or error (represented by the ellipses) in the final estimates is difficult to attribute to any individual sensor. (b) With the SCAAT method, uncertainty in final estimates can more easily be attributed to a particular individual sensor.</p> <p>Welch Thesis at 62.</p> <p>The Kalman filter operates in a predictor-corrector fashion, repeating a single time update and measurement update step whenever a new measurement vector becomes available. In the time update step the filter predicts what the state should be at the time of the measurements, based on the previous state estimate and a model of the process dynamics. In the measurement update step the filter uses the newly available measurement vector to correct the predicted state. In a normal implementation, depicted in figure 3.2, the time and measurement steps do not occur until all of the components of the measurement vector are available, i.e. until the state can be determined uniquely from the measurement vector. The measurement update step then processes the entire measurement vector in one batch, e.g. all three measurements in figure 3.2. This batch processing of the measurement data is relatively inflexible and can be computationally expensive if the measurement vector is large.</p> <p>Welch Thesis at 65.</p> <p>The use of a Kalman filter requires not only a dynamic model as described in section 4.2.1, but also a measurement model. The measurement model is used to predict the ideal noise-free response of each sensor and source pair, given the filter's current estimate of the target state as in equations (4.2) and (4.3). The prediction is then compared with an actual measurement, and the results are used to generate a correction for the filter's current estimate of the target state.</p> <p>Welch Thesis at 78.</p>

## Exhibit D-21

CLAIM 29	Welch Thesis
	<p>In light of the device isolation discussion in section 2.5.4 on page 61, the application of the above guidelines in the general case leads to the following heuristic for choosing the SCAAT Kalman filter measurement elements (constraints): During each SCAAT Kalman filter measurement update one should observe a single sensor and source pair only. Thus for the two-camera, four-beacon example, we could have immediately determined that each SCAAT Kalman filter measurement update should incorporate the (u,v) image coordinate of one beacon as seen in one camera. Each such observation could in fact be considered a single geometric constraint: the intersection of a line, the line from the beacon to the principal point of the camera lens, and a plane, the image plane.</p> <p>Welch Thesis at 81.</p>  <p><b>Figure 4.2:</b> Geometric view of state change during time update step. Per the derivatives in the state, the target is predicted to move and reorient since the time of the last filter estimate. Note that the target rotation is maintained incrementally in the state so the state orientation is zero before the time update and non-zero afterwards. The derivative elements of the state have been omitted and the spacial relationship exaggerated for clarity.</p> <p>Welch Thesis at 85.</p>



## Exhibit D-21

CLAIM 29	Welch Thesis
	<div data-bbox="525 243 1197 552">  <p> <math>P</math> = error covariance (density) before time update  <math>P^*</math> = error covariance (density) after time update  <math>= A(\delta t)P(t - \delta t)A^T(\delta t) + Q(\delta t)</math> </p> </div> <p data-bbox="525 568 1197 706"><b>Figure 4.3:</b> Geometric view of error covariance change during time update step. The change is shown by a growing probability density for each of <math>x</math>, <math>y</math>, and <math>z</math>. Note that reorientation is possible in general, but not for the dynamic model given in section 4.2.1. To visualize with Euclidean dimensions, the density has been limited to 3D: <math>x</math>, <math>y</math>, and <math>z</math> only. The shape, magnitude, and orientation are illustrative only.</p> <p data-bbox="525 722 1197 755">Welch Thesis at 85.</p> <p data-bbox="525 795 1375 1031">Continuing with the image-based measurement example, the situation is depicted in figure 4.8. The filter has some notion of where the target is located and how it is oriented, which determines its prediction of the measurement <math>\vec{\Delta z}</math> (the image coordinates of the known scene point). But the actual measurement <math>\hat{z}_\sigma(t)</math> indicates what the camera really “saw”. The difference between the two is the residual—the error in the measurement prediction.</p> <p data-bbox="525 1039 1197 1071">Welch Thesis at 92.</p>

## Exhibit D-21

CLAIM 29

Welch Thesis

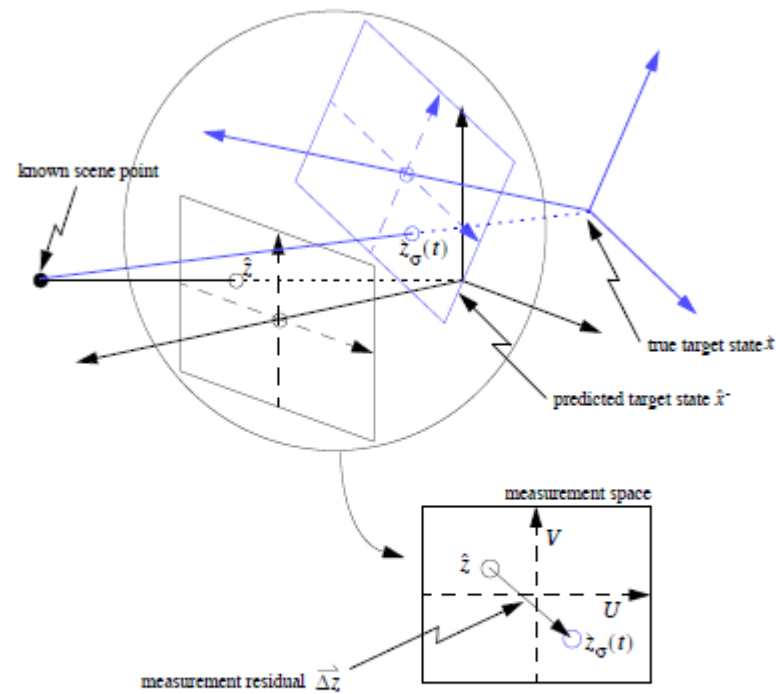


**Figure 4.8: The measurement residual.** Continuing with the image-based measurement example, the residual is the  $m_G$ -dimensional vector from the predicted measurement (image-plane coordinates)  $\hat{z}$  to the actual measurement  $\hat{z}_G(t)$ . The measurement prediction is what the filter thinks it will see given the predicted state, the actual measurement comes directly from the camera. (The relationship between the true and predicted state has been exaggerated for the purpose of illustration.)

Welch Thesis at 93.

## Exhibit D-21

## CLAIM 29

## Welch Thesis

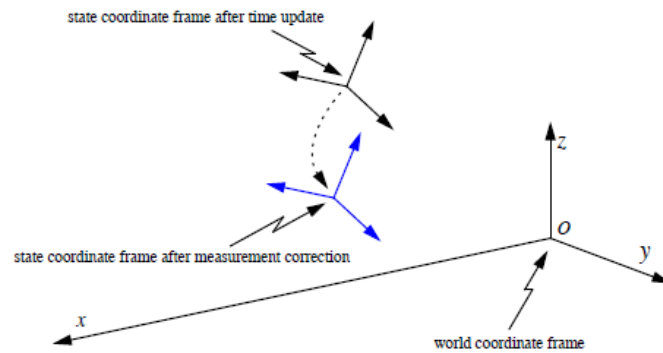


**Figure 4.9:** Geometric view of state change after measurement correction. Per the information in the measurement residual, the *a posteriori* state estimate is formed, i.e. the estimated target coordinate frame is moved and reoriented. Compare this with figure 4.2 on page 85. (Again the derivative elements of the state have been omitted and the spacial relationship exaggerated for clarity.)

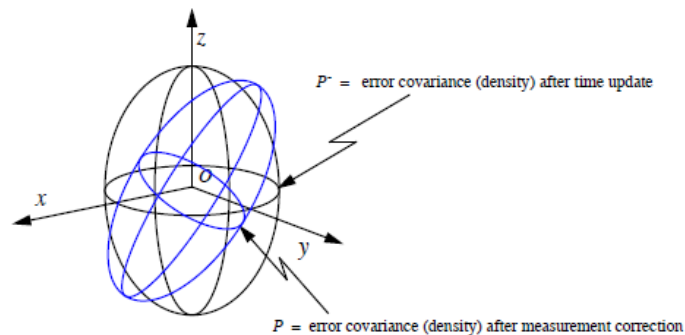


**Figure 4.10:** Geometric view of error covariance change after measurement update. The change is shown by a refined probability density for each of  $x$ ,  $y$ , and  $z$ . Note that in general the density is reoriented to reflect the constraint provided by the measurement. Compare this with figure 4.3 on page 85. (Again to visualize with Euclidean dimensions, the density has been limited to 3D:  $x$ ,  $y$ , and  $z$  only. The absolute shape, magnitude, and orientation are illustrative only.)

Welch Thesis at 95.

## Exhibit D-21

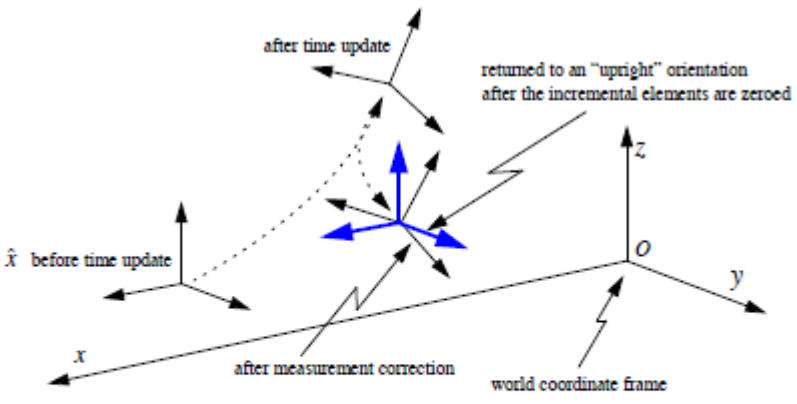
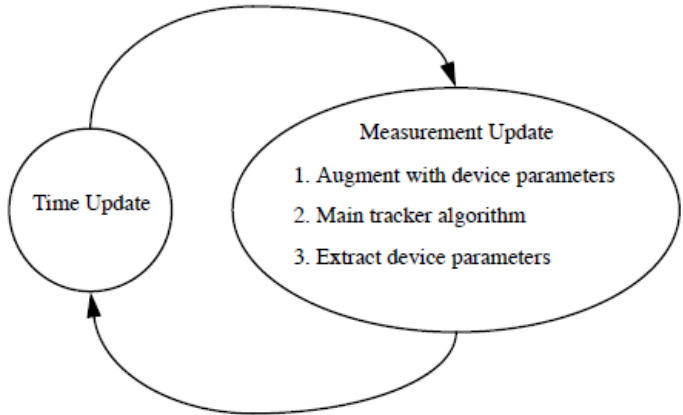
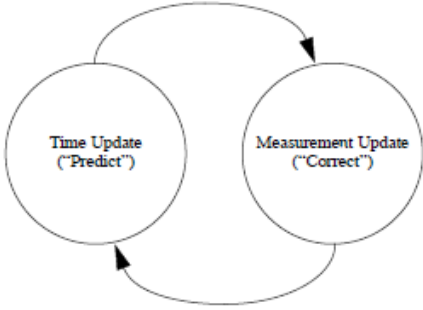
CLAIM 29	Welch Thesis
	 <p>Figure 4.11: Complete sequence of filter state coordinate frame transitions. This figure repeats the depictions in figures 4.2 and 4.9, and adds the final handling of the incremental rotations. After the measurement update, the incremental rotation is factored into the external orientation, and the incremental elements are zeroed in preparation for the next filter</p> <p>Welch Thesis at 97.</p>

Exhibit D-21

CLAIM 29	Welch Thesis
	<div data-bbox="667 245 1344 657"></div> <p data-bbox="573 672 1383 764"><b>Figure 4.12:</b> The revised tracking algorithm for autocalibration. The time update consists of equation (4.14). The measurement update consists of equations (4.24)-(4.27), then (4.15)-(4.22), and finally equation (4.28).</p> <p data-bbox="514 786 783 816">Welch Thesis at 102.</p> <p data-bbox="514 854 1961 1182">The Kalman filter estimates a process by using a form of feedback control: the filter estimates the process state at some time and then obtains feedback in the form of (noisy) measurements. As such, the equations for the Kalman filter fall into two groups: time update equations and measurement update equations. The time update equations are responsible for projecting forward (in time) the current state and error covariance estimates to obtain the a priori estimates for the next time step. The measurement update equations are responsible for the feedback—i.e. for incorporating a new measurement into the a priori estimate to obtain an improved a posteriori estimate. The time update equations can also be thought of as predictor equations, while the measurement update equations can be thought of as corrector equations. Indeed the final estimation algorithm resembles that of a predictor-corrector algorithm for solving numerical problems as shown in figure B.1.</p> <p data-bbox="514 1187 827 1218">Welch Thesis at 170-71.</p>

## Exhibit D-21

CLAIM 29	Welch Thesis
	 <p><b>Figure B.1:</b> The ongoing discrete Kalman filter cycle. The <i>time update</i> projects the current state estimate ahead in time. The <i>measurement update</i> adjusts the projected estimate by an actual measurement at that time. Notice the resemblance to a <i>predictor-corrector</i> algorithm</p> <p>Welch Thesis at 171.</p> <p>See also Welch Thesis Chapter 2.5 (describing autocalibration for sensor subsystems); Chapter 3.2 (describing sequential estimate updates performed by the SCAAT algorithm as new measurement data is collected by the system); Chapter 4.3 (use of the SCAAT algorithm for tracking to predict and correct sensor measurements); Chapter 4.4 (autocalibration using SCAAT algorithm); Chapter 6.1 (describing autocalibration of HiBall sensor system using SCAAT)</p> <p>See Disclosures with respect to Claim 1, <i>supra</i>; see also Defendants' Invalidity Contentions for further discussion.</p>

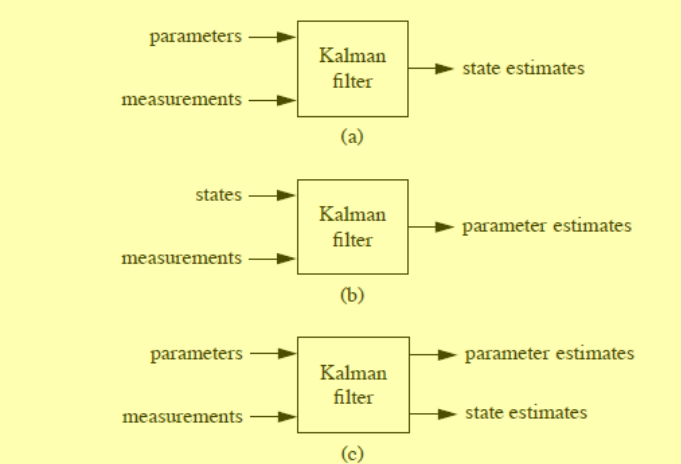
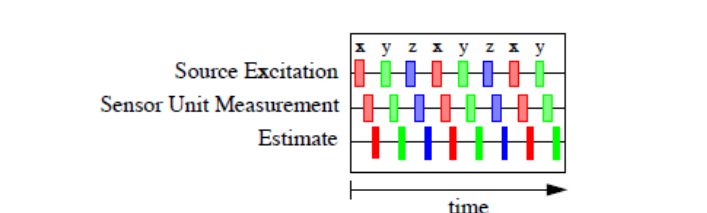
**K. INDEPENDENT CLAIM 47**

CLAIM 47	Welch Thesis
[47] A method of using multiple sensors in a tracking system comprising:	At least under Plaintiffs' apparent infringement theory, Welch Thesis discloses, either expressly or inherently, a method of using multiple sensors in a tracking system comprising: providing an estimation module; coupling one or more sensor modules to the estimation module, each associated with a different set of one or more sensors; configuring the tracking system, including providing configuration information from each of the sensor modules

## Exhibit D-21

CLAIM 47	Welch Thesis
<p>providing an estimation module;</p> <p>coupling one or more sensor modules to the estimation module, each associated with a different set of one or more sensors;</p> <p>configuring the tracking system, including</p> <p>providing configuration information from each of the sensor modules to the estimation module regarding the characteristics of the sensors associated with the sensor module, and</p> <p>configuring the estimation module using the provided configuration information;</p> <p>maintaining estimates of tracking parameters in the estimation module, including repeatedly</p>	<p>to the estimation module regarding the characteristics of the sensors associated with the sensor module, and configuring the estimation module using the provided configuration information; maintaining estimates of tracking parameters in the estimation module, including repeatedly passing data based on the estimates of the tracking parameters from the estimation module to one or more of the sensor modules, receiving from said one or more sensor modules at the estimation module data based on measurements obtained from the associated sensors, and the data passed to the sensor modules, and combining the data received from said one or more sensor modules and the estimates of the tracking parameters in the estimation module to update the tracking parameters. In the alternative, this element would be obvious over Welch Thesis in light of the other references disclosed in Defendants' Invalidity Contentions and/or the knowledge of one of ordinary skill in the art.</p> <p><i>See, e.g.:</i></p> <p><b>2.1.2 Data Fusion</b></p> <p>The Kalman filter assumes that the system being estimated has a <i>measurement equation</i> of the form given in equation (2.1) where the matrix <math>H(t_k)</math> relates the state vector <math>\hat{x}(t_k)</math> to the measurement vector <math>\hat{z}(t_k)</math>, and the vector <math>\vec{v}(t_k)</math> represents the measurement noise. Further details are presented in chapter 4 and can be found in Kalman filter texts such as [Brown92, Gelb74, Jacobs93, Lewis86].</p> $\hat{z}(t_k) = H(t_k)\hat{x}(t_k) + \vec{v}(t_k) \quad (2.1)$ <p>If the system being estimated has multiple forms of observation, there would be multiple corresponding measurement equations equation (2.1), i.e. multiple instances of the matrix <math>H(t_k)</math>, each representing a different relationship. By using the appropriate <math>H(t_k)</math> for each type of measurement, the filter effectively combines, blends, or <i>fuses</i> the information contained in the heterogeneous measurements.</p> <p>This capability for heterogeneous <i>data fusion</i>, combined with the properties discussed in section 2.1.1, has made the Kalman filter a very popular means of data fusion. For example the Kalman filter has been used for navigation [Geier87, Mahmoud94, Watanabe94], for virtual environment tracking [Azuma95, Emura94, Foxlin96], and for 3D scene modeling [Grandjean89, VanPabst95].</p> <p>Welch Thesis at 46.</p>

Exhibit D-21

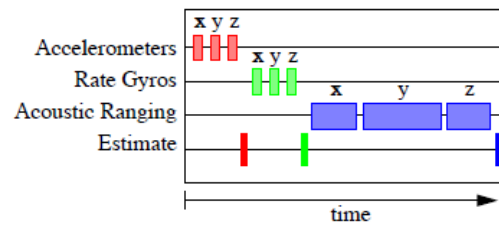
CLAIM 47	Welch Thesis
<p>passing data based on the estimates of the tracking parameters from the estimation module to one or more of the sensor modules,</p> <p>receiving from said one or more sensor modules at the estimation module data based on measurements obtained from the associated sensors, and the data passed to the sensor modules, and</p> <p>combining the data received from said one or more sensor modules and the estimates of the tracking parameters in the estimation module to update the tracking parameters.</p>	<div data-bbox="516 237 1192 876"><p data-bbox="516 714 1192 876"><b>Figure 2.2:</b> State versus parameter estimation. (a) The system parameters are known, and are used with the measurements to estimate the states. (b) For calibration purposes, known states can be used with measurements to estimate the system parameters. (c) A set of parameters can be used in conjunction with measurements to estimate another (not necessarily disjoint) set of parameters <i>and</i> the states.</p></div> <p data-bbox="516 893 768 933">Welch Thesis at 49.</p> <div data-bbox="516 950 1218 1161"></div> <p data-bbox="516 1177 1218 1258"><b>Figure 2.4:</b> Timing diagram for a (hypothetical) SCAAT magnetic tracker. The state estimate is updated after sensing each individual excitation vector.</p> <p data-bbox="516 1274 768 1315">Welch Thesis at 52.</p>



## Exhibit D-21

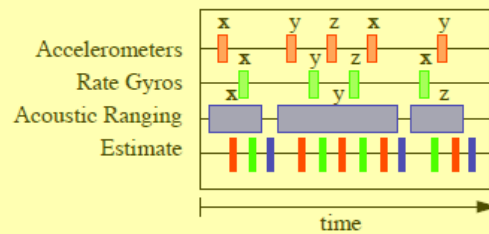
## CLAIM 47

## Welch Thesis



**Figure 2.7:** Timing diagram for a hypothetical conventional hybrid tracking system. The state estimate is updated only after each group of 3 homogeneous measurements.

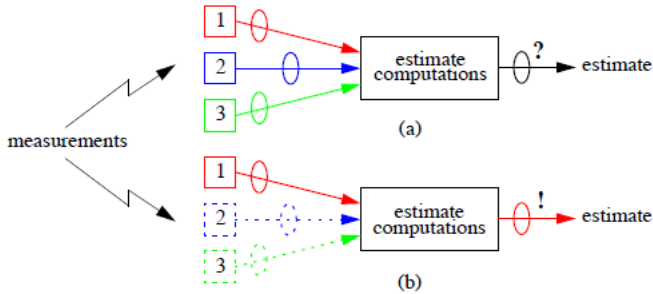
Welch Thesis at 57.



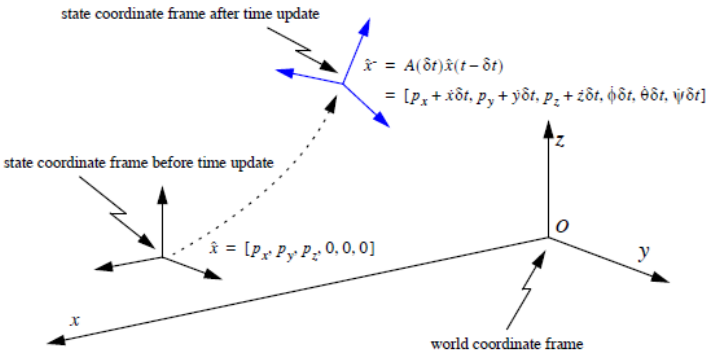
**Figure 2.8:** Timing diagram for a SCAAT inertial-acoustic hybrid tracking system. The state estimate is updated whenever an individual measurement becomes available.

Welch Thesis at 58.

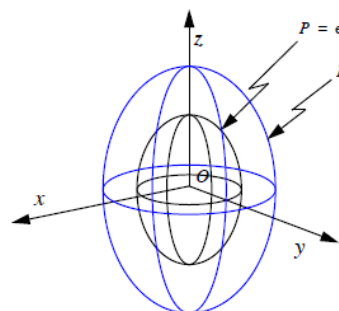
## Exhibit D-21

CLAIM 47	Welch Thesis
	 <p><b>Figure 2.11: Autocalibration and attribution of measurement error.</b> (a) Most algorithms operate on multiple measurements as a group, hence uncertainty or error (represented by the ellipses) in the final estimates is difficult to attribute to any individual sensor. (b) With the SCAAT method, uncertainty in final estimates can more easily be attributed to a particular individual sensor.</p> <p>Welch Thesis at 62.</p> <p>The Kalman filter operates in a predictor-corrector fashion, repeating a single time update and measurement update step whenever a new measurement vector becomes available. In the time update step the filter predicts what the state should be at the time of the measurements, based on the previous state estimate and a model of the process dynamics. In the measurement update step the filter uses the newly available measurement vector to correct the predicted state. In a normal implementation, depicted in figure 3.2, the time and measurement steps do not occur until all of the components of the measurement vector are available, i.e. until the state can be determined uniquely from the measurement vector. The measurement update step then processes the entire measurement vector in one batch, e.g. all three measurements in figure 3.2. This batch processing of the measurement data is relatively inflexible and can be computationally expensive if the measurement vector is large.</p> <p>Welch Thesis at 65.</p> <p>The use of a Kalman filter requires not only a dynamic model as described in section 4.2.1, but also a measurement model. The measurement model is used to predict the ideal noise-free response of each sensor and source pair, given the filter's current estimate of the target state as in equations (4.2) and (4.3). The prediction is then compared with an actual measurement, and the results are used to generate a correction for the filter's current estimate of the target state.</p> <p>Welch Thesis at 78.</p>

## Exhibit D-21

CLAIM 47	Welch Thesis
	<p>In light of the device isolation discussion in section 2.5.4 on page 61, the application of the above guidelines in the general case leads to the following heuristic for choosing the SCAAT Kalman filter measurement elements (constraints): During each SCAAT Kalman filter measurement update one should observe a single sensor and source pair only. Thus for the two-camera, four-beacon example, we could have immediately determined that each SCAAT Kalman filter measurement update should incorporate the (u,v) image coordinate of one beacon as seen in one camera. Each such observation could in fact be considered a single geometric constraint: the intersection of a line, the line from the beacon to the principal point of the camera lens, and a plane, the image plane.</p> <p>Welch Thesis at 81.</p>  <p><b>Figure 4.2:</b> Geometric view of state change during time update step. Per the derivatives in the state, the target is predicted to move and reorient since the time of the last filter estimate. Note that the target rotation is maintained incrementally in the state so the state orientation is zero before the time update and non-zero afterwards. The derivative elements of the state have been omitted and the spacial relationship exaggerated for clarity.</p> <p>Welch Thesis at 85.</p>

## Exhibit D-21

CLAIM 47	Welch Thesis
	<div data-bbox="525 243 1197 552">  <p> <math>P</math> = error covariance (density) before time update  <math>P^*</math> = error covariance (density) after time update  <math>= A(\delta t)P(t - \delta t)A^T(\delta t) + Q(\delta t)</math> </p> </div> <p data-bbox="525 568 1197 706"><b>Figure 4.3:</b> Geometric view of error covariance change during time update step. The change is shown by a growing probability density for each of <math>x</math>, <math>y</math>, and <math>z</math>. Note that reorientation is possible in general, but not for the dynamic model given in section 4.2.1. To visualize with Euclidean dimensions, the density has been limited to 3D: <math>x</math>, <math>y</math>, and <math>z</math> only. The shape, magnitude, and orientation are illustrative only.</p> <p data-bbox="525 722 1197 755">Welch Thesis at 85.</p> <p data-bbox="525 795 1375 1031">Continuing with the image-based measurement example, the situation is depicted in figure 4.8. The filter has some notion of where the target is located and how it is oriented, which determines its prediction of the measurement <math>\vec{\Delta z}</math> (the image coordinates of the known scene point). But the actual measurement <math>\hat{z}_\sigma(t)</math> indicates what the camera really “saw”. The difference between the two is the residual—the error in the measurement prediction.</p> <p data-bbox="525 1039 1197 1071">Welch Thesis at 92.</p>

## Exhibit D-21

CLAIM 47

Welch Thesis

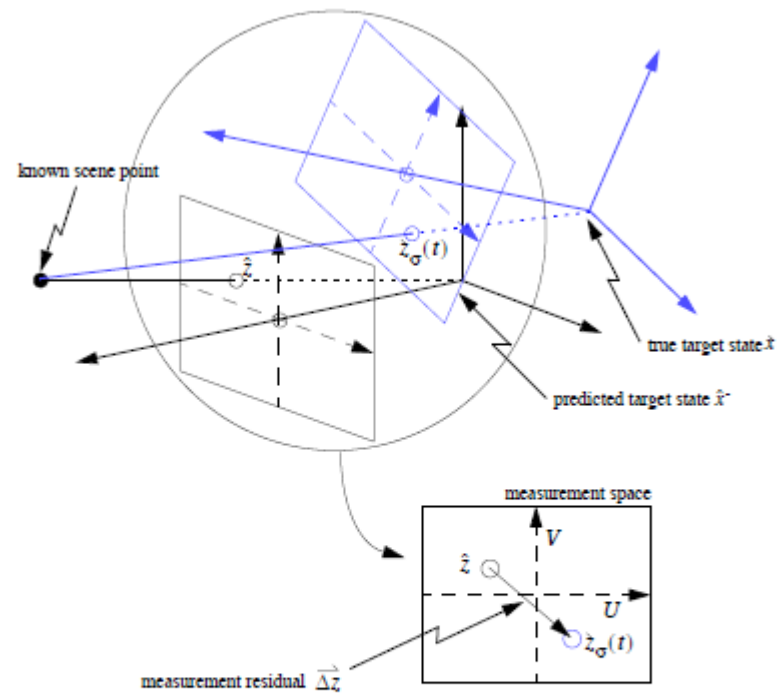


Figure 4.8: The measurement residual. Continuing with the image-based measurement example, the residual is the  $m_G$ -dimensional vector from the predicted measurement (image-plane coordinates)  $\hat{z}$  to the actual measurement  $\hat{z}_G(t)$ . The measurement prediction is what the filter thinks it will see given the predicted state, the actual measurement comes directly from the camera. (The relationship between the true and predicted state has been exaggerated for the purpose of illustration.)

Welch Thesis at 93.

## Exhibit D-21

## CLAIM 47

## Welch Thesis

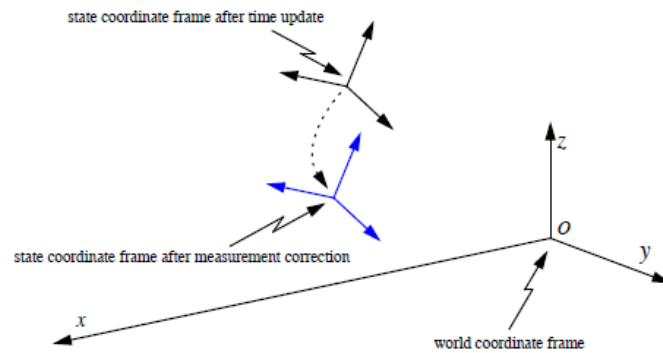


**Figure 4.9:** Geometric view of state change after measurement correction. Per the information in the measurement residual, the *a posteriori* state estimate is formed, i.e. the estimated target coordinate frame is moved and reoriented. Compare this with figure 4.2 on page 85. (Again the derivative elements of the state have been omitted and the spacial relationship exaggerated for clarity.)

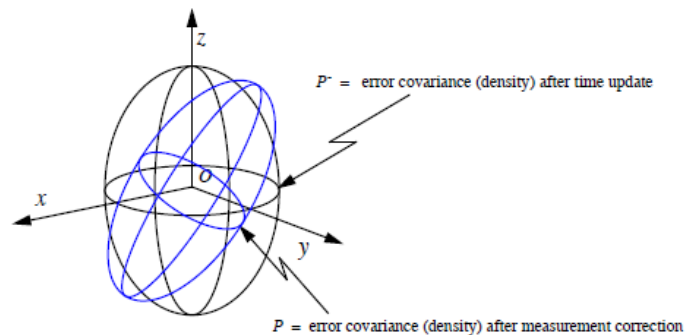


**Figure 4.10:** Geometric view of error covariance change after measurement update. The change is shown by a refined probability density for each of  $x$ ,  $y$ , and  $z$ . Note that in general the density is reoriented to reflect the constraint provided by the measurement. Compare this with figure 4.3 on page 85. (Again to visualize with Euclidean dimensions, the density has been limited to 3D:  $x$ ,  $y$ , and  $z$  only. The absolute shape, magnitude, and orientation are illustrative only.)

Welch Thesis at 95.

## Exhibit D-21

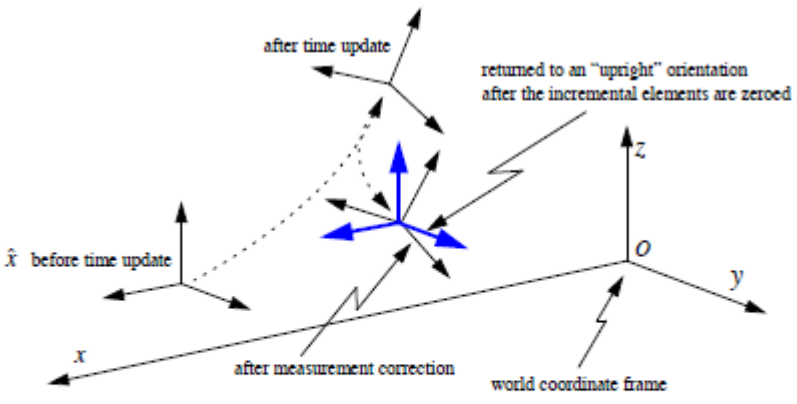
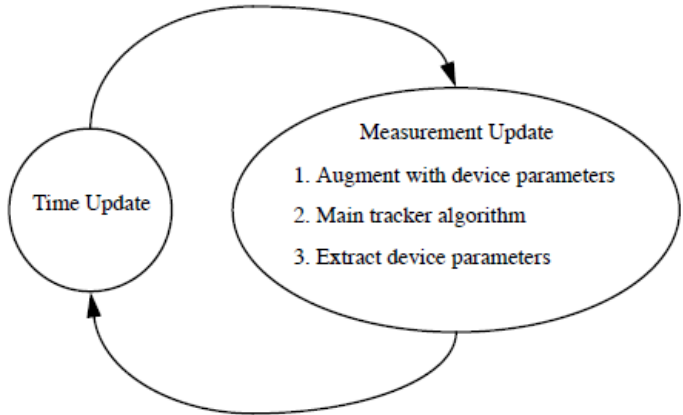
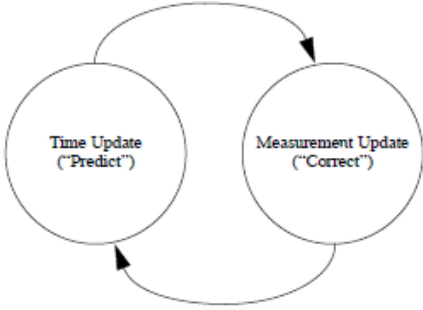
CLAIM 47	Welch Thesis
	 <p>Figure 4.11: Complete sequence of filter state coordinate frame transitions. This figure repeats the depictions in figures 4.2 and 4.9, and adds the final handling of the incremental rotations. After the measurement update, the incremental rotation is factored into the external orientation, and the incremental elements are zeroed in preparation for the next filter</p> <p>Welch Thesis at 97.</p>

Exhibit D-21

CLAIM 47	Welch Thesis
	<div data-bbox="667 245 1344 657"></div> <p data-bbox="573 672 1383 764"><b>Figure 4.12:</b> The revised tracking algorithm for autocalibration. The time update consists of equation (4.14). The measurement update consists of equations (4.24)-(4.27), then (4.15)-(4.22), and finally equation (4.28).</p> <p data-bbox="516 786 783 816">Welch Thesis at 102.</p> <p data-bbox="516 854 1961 1216"><b>The Kalman filter estimates a process by using a form of feedback control: the filter estimates the process state at some time and then obtains feedback in the form of (noisy) measurements. As such, the equations for the Kalman filter fall into two groups: time update equations and measurement update equations. The time update equations are responsible for projecting forward (in time) the current state and error covariance estimates to obtain the a priori estimates for the next time step.</b> The measurement update equations are responsible for the feedback—i.e. for incorporating a new measurement into the a priori estimate to obtain an improved a posteriori estimate. The time update equations can also be thought of as predictor equations, while the measurement update equations can be thought of as corrector equations. Indeed the final estimation algorithm resembles that of a predictor-corrector algorithm for solving numerical problems as shown in figure B.1.</p> <p data-bbox="516 1221 827 1252">Welch Thesis at 170-71.</p>



## Exhibit D-21

CLAIM 47	Welch Thesis
	 <p><b>Figure B.1:</b> The ongoing discrete Kalman filter cycle. The <i>time update</i> projects the current state estimate ahead in time. The <i>measurement update</i> adjusts the projected estimate by an actual measurement at that time. Notice the resemblance to a <i>predictor-corrector</i> algorithm</p> <p>Welch Thesis at 171.</p> <p><i>See also</i> Welch Thesis Chapter 2.5 (describing autocalibration for sensor subsystems); Chapter 3.2 (describing sequential estimate updates performed by the SCAAT algorithm as new measurement data is collected by the system); Chapter 4.3 (use of the SCAAT algorithm for tracking to predict and correct sensor measurements); Chapter 4.4 (autocalibration using SCAAT algorithm); Chapter 6.1 (describing autocalibration of HiBall sensor system using SCAAT)</p> <p><i>See also</i> Defendants' Invalidity Contentions for further discussion.</p>

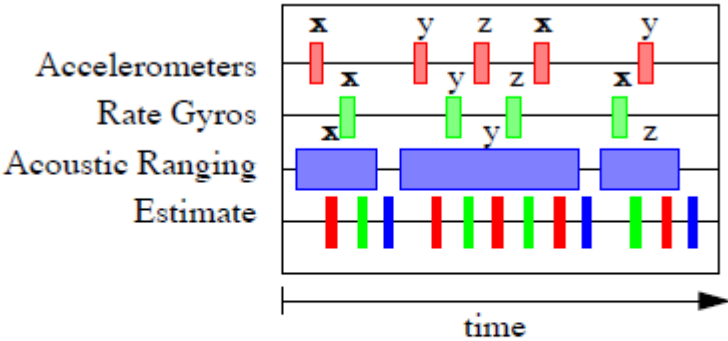
## L. DEPENDENT CLAIM 50

CLAIM 50	Welch Thesis
[50] The method of claim 47 wherein providing the estimation module includes	At least under Plaintiffs' apparent infringement theory, Welch Thesis discloses, either expressly or inherently, the method of claim 47 wherein providing the estimation module includes providing a module that is configurable to use different sets of sensor modules coupled to it. In the alternative, this element would be obvious over Welch

## Exhibit D-21

CLAIM 50	Welch Thesis
<p>providing a module that is configurable to use different sets of sensor modules coupled to it.</p>	<p>Thesis in light of the other references disclosed in Defendants' Invalidity Contentions and/or the knowledge of one of ordinary skill in the art.</p> <p><i>See, e.g.:</i></p> <p>For the sake of illustration, imagine an inertial-acoustical hybrid tracking system composed of three accelerometers, three rate gyros, and an acoustical line-of-sight system (to control drift from the inertial sensors). Note that not only will the acoustical measurements take longer than the inertial measurements, the acoustical measurement times will vary with distance between the source and sensors. A conventional method for data fusion might repeat the fixed pattern shown in figure 2.7. Notice that an estimate is produced only after collecting an orthogonal group of measurements from each (any one) subsystem.</p> <p>In contrast, a SCAAT implementation might interleave sensor measurements as depicted in figure 2.8. <b>Note the flexibility of measurement type, availability, rate, and ordering.</b> Again because an estimate is produced with every sensor measurement, latency is reduced and the estimation rate is increased.</p> <p>Welch Thesis at 58.</p> <div data-bbox="651 854 1417 1190" data-label="Figure"> <p>The figure is a timing diagram with four horizontal tracks labeled on the left: Accelerometers, Rate Gyros, Acoustic Ranging, and Estimate. A horizontal arrow at the bottom is labeled 'time'.    - Accelerometers: Three red vertical bars, each labeled 'x y z' above them.    - Rate Gyros: Three green vertical bars, each labeled 'x y z' above them.    - Acoustic Ranging: Three blue horizontal bars, each labeled 'x', 'y', and 'z' above them respectively.    - Estimate: Three vertical bars (red, green, and blue) corresponding to the completion of the measurement groups from Accelerometers, Rate Gyros, and Acoustic Ranging respectively.</p> </div> <p><b>Figure 2.7:</b> Timing diagram for a hypothetical conventional hybrid tracking system. The state estimate is updated only after each group of 3 homogeneous measurements.</p> <p>Welch Thesis at 58.</p>

Exhibit D-21

CLAIM 50	Welch Thesis
	<div data-bbox="688 264 1411 602"></div> <p data-bbox="531 630 1587 743"><b>Figure 2.8:</b> Timing diagram for a SCAAT inertial-acoustic hybrid tracking system. The state estimate is updated whenever an individual measurement becomes available.</p> <p data-bbox="514 776 768 808">Welch Thesis at 59.</p> <p data-bbox="514 846 1961 1170">Finally, I would like to see the SCAAT algorithm implemented in some other tracking systems beyond the UNC HiBall tracking system, for example the systems listed in table 2.2 on page 63. In particular, I would be interested in seeing the method applied to (1) magnetic tracking systems, e.g. the Polhemus Fastrak and the Ascension Bird, (2) a GPS navigation system, and (3) an computer-vision-based system. With respect to the magnetic systems, the implementation could be difficult because it’s not clear what level of measurement control or insight the general user has. A GPS implementation shows more promise as many modern receivers provide the user with access to relatively low-level measurement information [Kaplan96]. Finally, a computer-vision based system may be in the future as we (Bishop, Chi and Welch) are currently in the process of proposing a new inertial/optical hybrid tracker.</p> <p data-bbox="514 1175 827 1208">Welch Thesis at 159-60.</p> <p data-bbox="514 1245 1365 1278"><i>See also</i> Defendants’ Invalidity Contentions for further discussion.</p>

## Exhibit D-21

## M. DEPENDENT CLAIM 51

CLAIM 51	Welch Thesis
<p>[51] The method of claim 47 wherein maintaining estimates of the tracking parameters in the estimation module includes using a stochastic model in the estimation module.</p>	<p>At least under Plaintiffs' apparent infringement theory, Welch Thesis discloses, either expressly or inherently, the method of claim 47 wherein maintaining estimates of the tracking parameters in the estimation module includes using a stochastic model in the estimation module. In the alternative, this element would be obvious over Welch Thesis in light of the other references disclosed in Defendants' Invalidity Contentions and/or the knowledge of one of ordinary skill in the art.</p> <p><i>See, e.g.:</i></p> <p>The Kalman filter provides a powerful mathematical framework within which a minimum mean-square-error estimate of a user's position and orientation can be tracked using a sequence of <i>single</i> sensor observations, as opposed to <i>groups</i> of observations. We refer to this new approach as <i>single-constraint-at-a-time</i> or SCAAT tracking. The method improves accuracy by properly assimilating sequential observations, filtering sensor measurements, and by concurrently <i>autocalibrating</i> mechanical or electrical devices. The method facilitates user motion prediction, multisensor data fusion, and in systems where the observations are only available sequentially it provides estimates at a higher rate and with lower latency than a multiple-constraint approach.</p> <p>Improved accuracy is realized primarily for three reasons. First, the method avoids mathematically treating truly sequential observations as if they were simultaneous. Second, because each estimate is based on the observation of an individual device, perceived error (statistically unusual estimates) can be more directly attributed to the corresponding device. This can be used for concurrent autocalibration which can be elegantly incorporated into the existing Kalman filter. <b>Third, the Kalman filter inherently addresses the effects of noisy device measurements. Beyond accuracy, the method nicely facilitates motion prediction because the Kalman filter already incorporates a model of the user's dynamics, and because it provides smoothed estimates of the user state, including potentially unmeasured elements.</b> Finally, in systems where the observations are only available sequentially, the method can be used to weave together information from individual devices in a very flexible manner, producing a new estimate as soon as each individual observation becomes available, thus facilitating multisensor data fusion and improving the estimate rates and latencies.</p> <p>Welch Thesis at Abstract.</p> <p>A Kalman filter can be used to estimate a globally-observable process by sequentially incorporating only measurements of locally-unobservable processes. The use of a Kalman filter in such a manner offers several</p>

## Exhibit D-21

CLAIM 51	Welch Thesis
	<p>advantages: (1) a flexible framework for heterogeneous multisensor data fusion; (2) a unique opportunity to perform concurrent device autocalibration; and in a system that allows only sequential measurements, (3) significantly improved estimate rates and latencies; and (4) avoidance of the incorrect simultaneity assumption. Welch Thesis at 43.</p> <p>There are four typical reasons why people employ Kalman filters in systems where a signal (often continuous) is to be estimated with a sequence of discrete measurements or observations: (1) filtering; (2) data fusion; (3) prediction; and (4) calibration. Welch Thesis at 44.</p> <p><b>The Kalman filter is a set of mathematical equations that provides an efficient computational (recursive) means of using noisy measurements to estimate the state of a linear system, while minimizing the expected mean-squared estimation error.</b> Welch Thesis at 45.</p> <p><b>The Kalman filter is generally presented as a way of estimating values of stochastic variables (the states) of linear systems whose associated system parameters (e.g. model dynamics and noise characteristics) have known values.</b> Interestingly enough, the filter can just as well be turned around and used to estimate values of unknown system parameters when the states are known [Jacobs93]. In fact, it can even be used to estimate both system states and parameters as represented in figure 2.2.</p> <p>In particular, the characteristics outlined in sections 2.1.1 and 2.1.2 make the Kalman filter an attractive and popular option for calibration. Referring to figure 2.2, the situation depicted in (a) is that of a Kalman filter being used only to estimate the system states, i.e. there is no calibration. Examples of the situation depicted in (b) include [Wefald84] and [Foxlin96]. Recent examples of the situation depicted in (c) include [Azarbayejani95] and the work presented in this dissertation. Welch Thesis at 48.</p>

Exhibit D-21

CLAIM 51	Welch Thesis
	<div><p>(a)</p><p>(b)</p><p>(c)</p></div> <p><b>Figure 2.2:</b> State versus parameter estimation. (a) The system parameters are known, and are used with the measurements to estimate the states. (b) For calibration purposes, known states can be used with measurements to estimate the system parameters. (c) A set of parameters can be used in conjunction with measurements to estimate another (not necessarily disjoint) set of parameters <i>and</i> the states.</p> <p>Welch Thesis at 49.</p> <p>Beyond tracking or navigation, the SCAAT method can be applied to any situation where stochastic estimation is desired, and multiple measurements (simultaneous or not) are used to form a complete estimate. Some examples are real-time or off-line state estimation, parameter estimation [Lewis86], and generalized data fusion or assimilation (e.g. see [Watanabe94, VanPabst95, Grandjean89, Mahmoud94, Ikeda95]). As such I believe that this method may prove to be of interest to the larger scientific and engineering community in addressing a more general class of tracking and estimation problems.</p> <p>Welch Thesis at 62.</p> <p>Given a set of unknowns, and a set of equations (linear or nonlinear) that simultaneously describe a known relationship between the unknowns, several methods exist for solving for the unknowns. For several examples, see [Press90]. The Kalman filter can also be used to estimate the unknowns by mapping the given equations and</p>

## Exhibit D-21

CLAIM 51	Welch Thesis
	<p>constraints into the Kalman filter framework. Furthermore, I believe that it would be interesting to investigate the application of the SCAAT method to this problem. Welch Thesis at 158</p> <p><i>See also</i> Welch Thesis Chapter 4 (describing implementation of Kalman filter in the SCAAT tracking method); Welch Thesis Appendix B (providing a “ready and accessible introduction to both the discrete Kalman filter and the extended Kalman filter).</p> <p><i>See</i> Defendants’ Invalidity Contentions for further discussion.</p>

## N. DEPENDENT CLAIM 52

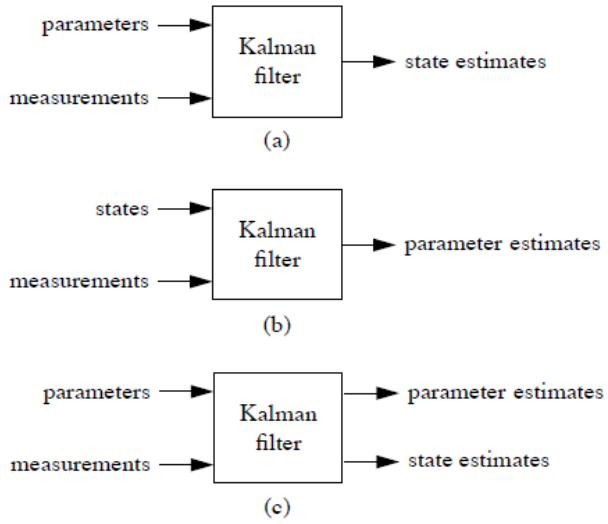
CLAIM 52	Welch Thesis
<p>[52] The method of claim 51 wherein using a stochastic model includes implementing some or all of a Kalman filter in the estimation module.</p>	<p>At least under Plaintiffs’ apparent infringement theory, Welch Thesis discloses, either expressly or inherently, the method of claim 51 wherein using a stochastic model includes implementing some or all of a Kalman filter in the estimation module. In the alternative, this element would be obvious over Welch Thesis in light of the other references disclosed in Defendants’ Invalidity Contentions and/or the knowledge of one of ordinary skill in the art.</p> <p><i>See, e.g.:</i></p> <p><b>The Kalman filter</b> provides a powerful mathematical framework within which a minimum mean-square-error estimate of a user’s position and orientation can be tracked using a sequence of <i>single</i> sensor observations, as opposed to <i>groups</i> of observations. We refer to this new approach as <i>single-constraint-at-a-time</i> or SCAAT tracking. The method improves accuracy by properly assimilating sequential observations, filtering sensor measurements, and by concurrently <i>autocalibrating</i> mechanical or electrical devices. The method facilitates user motion prediction, multisensor data fusion, and in systems where the observations are only available sequentially it provides estimates at a higher rate and with lower latency than a multiple-constraint approach.</p> <p>Improved accuracy is realized primarily for three reasons. First, the method avoids mathematically treating truly sequential observations as if they were simultaneous. Second, because each estimate is based on the observation of an individual device, perceived error (statistically unusual estimates) can be more directly attributed to the</p>

## Exhibit D-21

CLAIM 52	Welch Thesis
	<p>corresponding device. This can be used for concurrent autocalibration which can be elegantly incorporated into the existing Kalman filter. <b>Third, the Kalman filter inherently addresses the effects of noisy device measurements.</b> Beyond accuracy, the method nicely facilitates motion prediction because the Kalman filter already incorporates a model of the user's dynamics, and because it provides smoothed estimates of the user state, including potentially unmeasured elements. Finally, in systems where the observations are only available sequentially, the method can be used to weave together information from individual devices in a very flexible manner, producing a new estimate as soon as each individual observation becomes available, thus facilitating multisensor data fusion and improving the estimate rates and latencies.</p> <p>Welch Thesis at Abstract.</p> <p>A Kalman filter can be used to estimate a globally-observable process by sequentially incorporating only measurements of locally-unobservable processes. The use of a Kalman filter in such a manner offers several advantages: (1) a flexible framework for heterogeneous multisensor data fusion; (2) a unique opportunity to perform concurrent device autocalibration; and in a system that allows only sequential measurements, (3) significantly improved estimate rates and latencies; and (4) avoidance of the incorrect simultaneity assumption.</p> <p>Welch Thesis at 43.</p> <p>There are four typical reasons why people employ Kalman filters in systems where a signal (often continuous) is to be estimated with a sequence of discrete measurements or observations: (1) filtering; (2) data fusion; (3) prediction; and (4) calibration.</p> <p>Welch Thesis at 44.</p> <p>The Kalman filter is a set of mathematical equations that provides an efficient computational (recursive) means of using noisy measurements to estimate the state of a linear system, while minimizing the expected mean-squared estimation error.</p> <p>Welch Thesis at 45.</p> <p><b>The Kalman filter is generally presented as a way of estimating values of stochastic variables</b> (the states) of linear systems whose associated system parameters (e.g. model dynamics and noise characteristics) have known values. Interestingly enough, the filter can just as well be turned around and used to estimate values of unknown system parameters when the states are known [Jacobs93]. In fact, it can even be used to estimate both system states and parameters as represented in figure 2.2.</p>



## Exhibit D-21

CLAIM 52	Welch Thesis
	<p>In particular, the characteristics outlined in sections 2.1.1 and 2.1.2 make the Kalman filter an attractive and popular option for calibration. Referring to figure 2.2, the situation depicted in (a) is that of a Kalman filter being used only to estimate the system states, i.e. there is no calibration. Examples of the situation depicted in (b) include [Wefald84] and [Foxlin96]. Recent examples of the situation depicted in (c) include [Azarbayejani95] and the work presented in this dissertation.</p> <p>Welch Thesis at 48.</p>  <p><b>Figure 2.2:</b> State versus parameter estimation. (a) The system parameters are known, and are used with the measurements to estimate the states. (b) For calibration purposes, known states can be used with measurements to estimate the system parameters. (c) A set of parameters can be used in conjunction with measurements to estimate another (not necessarily disjoint) set of parameters <i>and</i> the states.</p> <p>Welch Thesis at 49.</p> <p>Given a set of unknowns, and a set of equations (linear or nonlinear) that simultaneously describe a known relationship between the unknowns, several methods exist for solving for the unknowns. For several examples, see [Press90]. The Kalman filter can also be used to estimate the unknowns by mapping the given equations and constraints into the Kalman filter framework. Furthermore, I believe that it would be interesting to investigate the</p>

## Exhibit D-21

CLAIM 52	Welch Thesis
	<p>application of the SCAAT method to this problem. Welch Thesis at 158</p> <p><i>See also</i> Welch Thesis Chapter 4 (describing implementation of Kalman filter in the SCAAT tracking method); Welch Thesis Appendix B (providing a “ready and accessible introduction to both the discrete Kalman filter and the extended Kalman filter).</p> <p><i>See also</i> Defendants’ Invalidity Contentions for further discussion.</p>

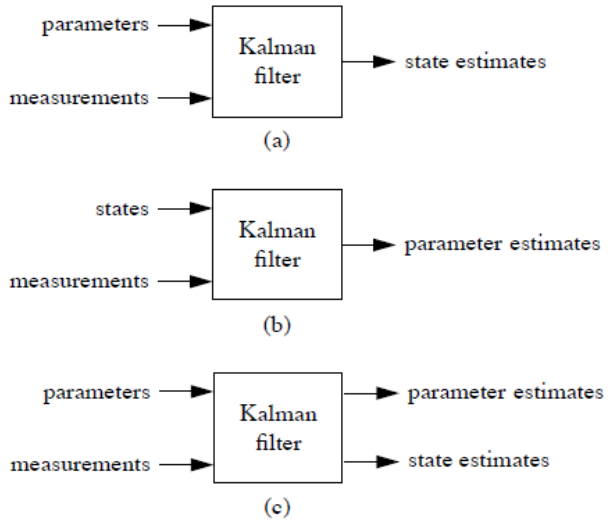
**O. DEPENDENT CLAIM 53**

CLAIM 53	Welch Thesis
<p>[53] The method of claim 52 wherein implementing some or all of the Kalman filter includes updating error estimates using linearized models of the sensor system.</p>	<p>At least under Plaintiffs’ apparent infringement theory, Welch Thesis discloses, either expressly or inherently, the method of claim 52 wherein implementing some or all of the Kalman filter includes updating error estimates using linearized models of the sensor system. In the alternative, this element would be obvious over Welch Thesis in light of the other references disclosed in Defendants’ Invalidity Contentions and/or the knowledge of one of ordinary skill in the art.</p> <p><i>See, e.g.:</i></p> <p>The Kalman filter provides a powerful mathematical framework within which a minimum mean-square-error estimate of a user’s position and orientation can be tracked using a sequence of <i>single</i> sensor observations, as opposed to <i>groups</i> of observations. We refer to this new approach as <i>single-constraint-at-a-time</i> or SCAAT tracking. The method improves accuracy by properly assimilating sequential observations, filtering sensor measurements, and by concurrently <i>autocalibrating</i> mechanical or electrical devices. The method facilitates user motion prediction, multisensor data fusion, and in systems where the observations are only available sequentially it provides estimates at a higher rate and with lower latency than a multiple-constraint approach.</p> <p>Improved accuracy is realized primarily for three reasons. First, the method avoids mathematically treating truly sequential observations as if they were simultaneous. Second, because each estimate is based on the observation of an individual device, perceived error (statistically unusual estimates) can be more directly attributed to the</p>

## Exhibit D-21

CLAIM 53	Welch Thesis
	<p>corresponding device. This can be used for concurrent autocalibration which can be elegantly incorporated into the existing Kalman filter. Third, the Kalman filter inherently addresses the effects of noisy device measurements. Beyond accuracy, the method nicely facilitates motion prediction because the Kalman filter already incorporates a model of the user's dynamics, and because it provides smoothed estimates of the user state, including potentially unmeasured elements. Finally, in systems where the observations are only available sequentially, the method can be used to weave together information from individual devices in a very flexible manner, producing a new estimate as soon as each individual observation becomes available, thus facilitating multisensor data fusion and improving the estimate rates and latencies. Welch Thesis at Abstract.</p> <p>A Kalman filter can be used to estimate a globally-observable process by sequentially incorporating only measurements of locally-unobservable processes. The use of a Kalman filter in such a manner offers several advantages: (1) a flexible framework for heterogeneous multisensor data fusion; (2) a unique opportunity to perform concurrent device autocalibration; and in a system that allows only sequential measurements, (3) significantly improved estimate rates and latencies; and (4) avoidance of the incorrect simultaneity assumption. Welch Thesis at 43.</p> <p>There are four typical reasons why people employ Kalman filters in systems where a signal (often continuous) is to be estimated with a sequence of discrete measurements or observations: (1) filtering; (2) data fusion; (3) prediction; and (4) calibration. Welch Thesis at 44.</p> <p><b>The Kalman filter is a set of mathematical equations that provides an efficient computational (recursive) means of using noisy measurements to estimate the state of a linear system,</b> while minimizing the expected mean-squared estimation error. Welch Thesis at 45.</p> <p><b>The Kalman filter is generally presented as a way of estimating values of stochastic variables (the states) of linear systems whose associated system parameters (e.g. model dynamics and noise characteristics) have known values.</b> Interestingly enough, the filter can just as well be turned around and used to estimate values of unknown system parameters when the states are known [Jacobs93]. In fact, it can even be used to estimate both system states and parameters as represented in figure 2.2.</p>

## Exhibit D-21

CLAIM 53	Welch Thesis
	<p>In particular, the characteristics outlined in sections 2.1.1 and 2.1.2 make the Kalman filter an attractive and popular option for calibration. Referring to figure 2.2, the situation depicted in (a) is that of a Kalman filter being used only to estimate the system states, i.e. there is no calibration. Examples of the situation depicted in (b) include [Wefald84] and [Foxlin96]. Recent examples of the situation depicted in (c) include [Azarbajejani95] and the work presented in this dissertation.</p> <p>Welch Thesis at 48.</p>  <p><b>Figure 2.2:</b> State versus parameter estimation. (a) The system parameters are known, and are used with the measurements to estimate the states. (b) For calibration purposes, known states can be used with measurements to estimate the system parameters. (c) A set of parameters can be used in conjunction with measurements to estimate another (not necessarily disjoint) set of parameters <i>and</i> the states.</p> <p>Welch Thesis at 49.</p> <p><b>Given a set of unknowns, and a set of equations (linear or nonlinear) that simultaneously describe a known relationship between the unknowns, several methods exist for solving for the unknowns.</b> For several examples, see [Press90]. The Kalman filter can also be used to estimate the unknowns by mapping the given equations and constraints into the Kalman filter framework. Furthermore, I believe that it would be interesting to</p>

## Exhibit D-21

CLAIM 53	Welch Thesis
	<p>investigate the application of the SCAAT method to this problem. Welch Thesis at 158</p> <p><i>See also</i> Welch Thesis Chapter 4 (describing implementation of Kalman filter in the SCAAT tracking method); Welch Thesis Appendix B (providing a “ready and accessible introduction to both the discrete Kalman filter and the extended Kalman filter).</p> <p>Possibly the most significant (and obvious) concern with respect to a SCAAT filter is its stability. <b>A linear system is said to be stable if its response to any input tends to a finite steady value after the input is removed [Jacobs93]. For the Kalman filter in general this is certainly not a new concern,</b> and there are standard requirements and corresponding tests that ensure or detect stability. Welch Thesis at 108</p> <p><b>The linear system associated with any single SCAAT observation can be viewed alone as a distinct time-invariant system.</b> In section 1.2 I stated that each such system in a SCAAT implementation is locally unobservable. From linear system theory (see [Maybeck70] p. 48) we know that a general necessary and sufficient condition for observability of a time-invariant linear system is that the observability matrix of equation (5.1) must have rank <math>n</math>, where <math>n</math> is the dimension of the state.</p> $M \equiv \begin{bmatrix} H^T & A^T H^T & \dots & (A^T)^{n-1} H^T \end{bmatrix}$ <p>Welch Thesis at 108-09</p> <p><i>See also</i> Defendants’ Invalidity Contentions for further discussion.</p>

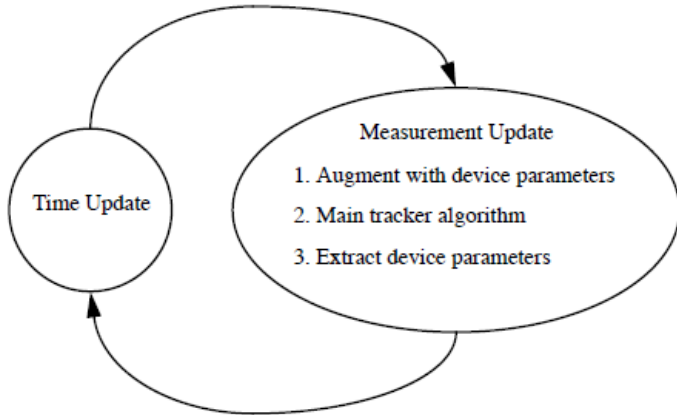
## P. DEPENDENT CLAIM 59

CLAIM 59	Welch Thesis
[59] The method of claim 47 wherein	At least under Plaintiffs’ apparent infringement theory, Welch Thesis discloses, either expressly or inherently, the method of claim 47 wherein providing configuration information from the sensor modules includes providing

## Exhibit D-21

CLAIM 59	Welch Thesis
<p>providing configuration information from the sensor modules includes providing information characterizing a type of a sensor associated with a sensor module.</p>	<p>information characterizing a type of a sensor associated with a sensor module. In the alternative, this element would be obvious over Welch Thesis in light of the other references disclosed in Defendants' Invalidity Contentions and/or the knowledge of one of ordinary skill in the art.</p> <p><i>See, e.g.:</i></p> <p style="padding-left: 40px;">Given an initial state estimate <math>\hat{x}(0)</math>, external orientation estimate <math>\hat{\alpha}(0)</math>, and error covariance estimate <math>P(0)</math>, the SCAAT algorithm proceeds similarly to a conventional EKF. For each measurement <math>\hat{z}_{\sigma}(t)</math> at time <math>t</math>, from some sensor of type <math>\sigma</math> and corresponding source, we cycle through the following update steps:</p> <p>Welch Thesis at 97.</p> <p>For the initial UNC HiBall tracking system implementation, and hence for these simulations, there is only one sensor type : a HiBall camera (photodiode). Therefore there is only a need for a single measurement function equation (4.10) to predict the measurement in equation (4.15). Welch Thesis at 123.</p>

## Exhibit D-21

CLAIM 59	Welch Thesis
	 <p><b>Figure 4.12:</b> The revised tracking algorithm for autocalibration. The time update consists of equation (4.14). The measurement update consists of equations (4.24)-(4.27), then (4.15)-(4.22), and finally equation (4.28).</p> <p>Welch Thesis at 102.</p> <p><i>See also</i> Welch Thesis Chapter 4.4 (autocalibration using SCAAT algorithm).</p> <p><i>See also</i> Defendants' Invalidity Contentions for further discussion.</p>

**Q. DEPENDENT CLAIM 60**

CLAIM 60	Welch Thesis
<p>[60] The method of claim 47 wherein providing configuration information from the sensor modules includes providing information characterizing a position</p>	<p>At least under Plaintiffs' apparent infringement theory, Welch Thesis discloses, either expressly or inherently, the method of claim 47 wherein providing configuration information from the sensor modules includes providing information characterizing a position or an orientation of a sensor associated with a sensor module. In the alternative, this element would be obvious over Welch Thesis in light of the other references disclosed in Defendants' Invalidity Contentions and/or the knowledge of one of ordinary skill in the art.</p> <p><i>See, e.g.:</i></p>

## Exhibit D-21

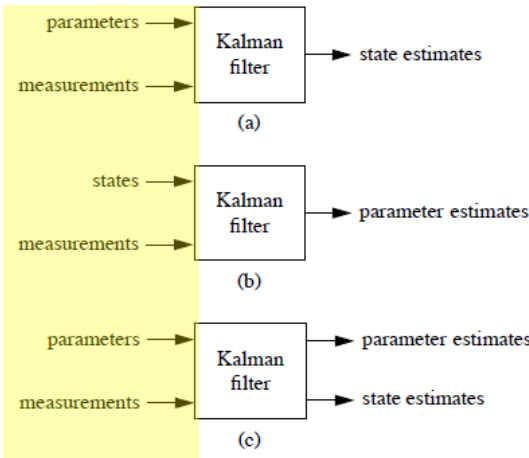
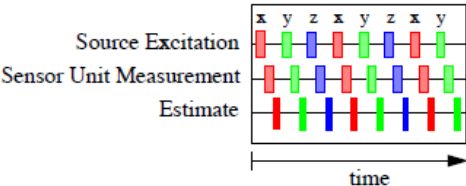
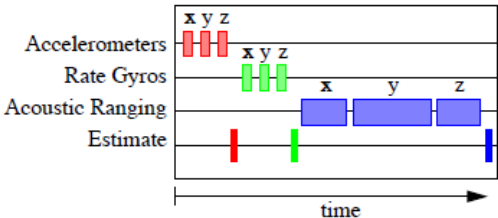
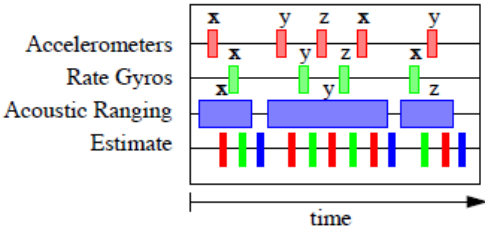
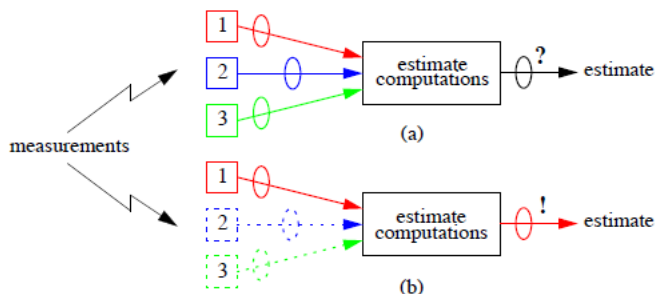
CLAIM 60	Welch Thesis
<p>or an orientation of a sensor associated with a sensor module.</p>	<p>The Kalman filter provides a powerful mathematical framework within which a minimum mean-square-error estimate of a user's position and orientation can be tracked using a sequence of single sensor observations, as opposed to groups of observations. We refer to this new approach as single-constraint-at-a-time or SCAAT tracking. The method <b>improves accuracy by properly assimilating sequential observations, filtering sensor measurements, and by concurrently autocalibrating mechanical or electrical devices</b>. The method facilitates user motion prediction, multisensor data fusion, and in systems where the observations are only available sequentially it provides estimates at a higher rate and with lower latency than a multiple-constraint approach. Welch Thesis at Abstract.</p>  <p>Figure 2.2: State versus parameter estimation. (a) The system parameters are known, and are used with the measurements to estimate the states. (b) For calibration purposes, known states can be used with measurements to estimate the system parameters. (c) A set of parameters can be used in conjunction with measurements to estimate another (not necessarily disjoint) set of parameters and the states.</p> <p>Welch Thesis at 49.</p>



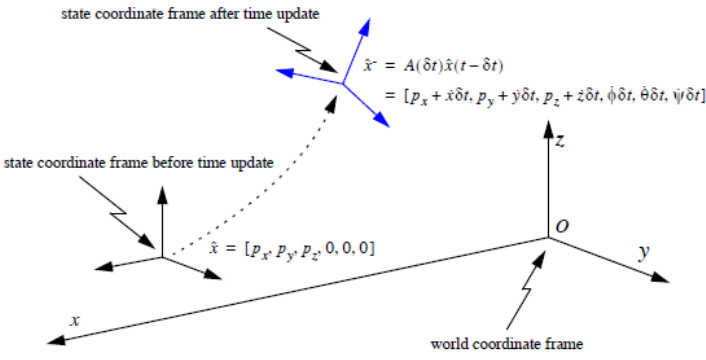
Exhibit D-21

CLAIM 60	Welch Thesis
	<div data-bbox="615 251 1077 435"></div> <div data-bbox="533 451 1218 529"><p><b>Figure 2.4:</b> Timing diagram for a (hypothetical) SCAAT magnetic tracker. The state estimate is updated after sensing each individual excitation vector.</p></div> <p data-bbox="516 553 768 584">Welch Thesis at 52.</p> <div data-bbox="621 630 1115 846"></div> <div data-bbox="539 862 1218 940"><p><b>Figure 2.7:</b> Timing diagram for a hypothetical conventional hybrid tracking system. The state estimate is updated only after each group of 3 homogeneous measurements.</p></div> <p data-bbox="516 953 768 984">Welch Thesis at 57.</p> <div data-bbox="667 1029 1148 1255"></div> <div data-bbox="562 1271 1266 1349"><p><b>Figure 2.8:</b> Timing diagram for a SCAAT inertial-acoustic hybrid tracking system. The state estimate is updated whenever an individual measurement becomes available.</p></div> <p data-bbox="516 1378 768 1409">Welch Thesis at 58.</p>

## Exhibit D-21

CLAIM 60	Welch Thesis
	 <p data-bbox="525 552 1176 698"><b>Figure 2.11: Autocalibration and attribution of measurement error.</b> (a) Most algorithms operate on multiple measurements as a group, hence uncertainty or error (represented by the ellipses) in the final estimates is difficult to attribute to any individual sensor. (b) With the SCAAT method, uncertainty in final estimates can more easily be attributed to a particular individual sensor.</p> <p data-bbox="514 706 766 738">Welch Thesis at 62.</p> <p data-bbox="514 771 1974 1136">The Kalman filter operates in a predictor-corrector fashion, repeating a single time update and measurement update step whenever a new measurement vector becomes available. In the time update step the filter predicts what the state should be at the time of the measurements, based on the previous state estimate and a model of the process dynamics. In the measurement update step the filter uses the newly available measurement vector to correct the predicted state. In a normal implementation, depicted in figure 3.2, the time and measurement steps do not occur until all of the components of the measurement vector are available, i.e. until the state can be determined uniquely from the measurement vector. <b>The measurement update step then processes the entire measurement vector in one batch, e.g. all three measurements in figure 3.2.</b> This batch processing of the measurement data is relatively inflexible and can be computationally expensive if the measurement vector is large.</p> <p data-bbox="514 1144 766 1177">Welch Thesis at 65.</p> <p data-bbox="514 1209 1974 1388">The use of a Kalman filter requires not only a dynamic model as described in section 4.2.1, but also a measurement model. The measurement model is used to predict the ideal noise-free response of each sensor and source pair, given the filter's current estimate of the target state as in equations (4.2) and (4.3). The prediction is then compared with an actual measurement, and the results are used to generate a correction for the filter's current estimate of the target state.</p> <p data-bbox="514 1396 766 1429">Welch Thesis at 78.</p>

## Exhibit D-21

CLAIM 60	Welch Thesis
	<p>In light of the device isolation discussion in section 2.5.4 on page 61, the application of the above guidelines in the general case leads to the following heuristic for choosing the SCAAT Kalman filter measurement elements (constraints): During each SCAAT Kalman filter measurement update one should observe a single sensor and source pair only. Thus for the two-camera, four-beacon example, we could have immediately determined that each SCAAT Kalman filter measurement update should incorporate the (u,v) image coordinate of one beacon as seen in one camera. Each such observation could in fact be considered a single geometric constraint: the intersection of a line, the line from the beacon to the principal point of the camera lens, and a plane, the image plane.</p> <p>Welch Thesis at 81.</p>  <p><b>Figure 4.2:</b> Geometric view of state change during time update step. Per the derivatives in the state, the target is predicted to move and reorient since the time of the last filter estimate. Note that the target rotation is maintained incrementally in the state so the state orientation is zero before the time update and non-zero afterwards. The derivative elements of the state have been omitted and the spacial relationship exaggerated for clarity.</p> <p>Welch Thesis at 85.</p>

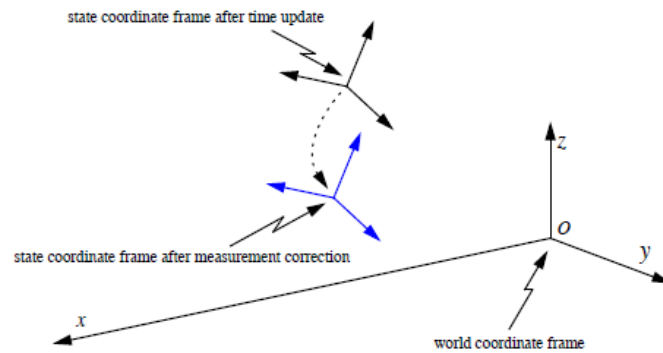
## Exhibit D-21

CLAIM 60	Welch Thesis
	<div data-bbox="525 243 1197 552"> <p> <math>P</math> = error covariance (density) before time update  <math>P^+</math> = error covariance (density) after time update  <math>= A(\delta t)P(t - \delta t)A^T(\delta t) + Q(\delta t)</math> </p> </div> <p> <b>Figure 4.3:</b> Geometric view of error covariance change during time update step. The change is shown by a growing probability density for each of <math>x</math>, <math>y</math>, and <math>z</math>. Note that reorientation is possible in general, but not for the dynamic model given in section 4.2.1. To visualize with Euclidean dimensions, the density has been limited to 3D: <math>x</math>, <math>y</math>, and <math>z</math> only. The shape, magnitude, and orientation are illustrative only.         </p> <p>Welch Thesis at 85.</p>

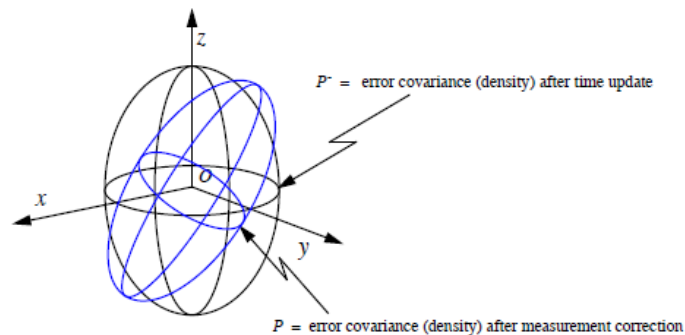
## Exhibit D-21

## CLAIM 60

## Welch Thesis



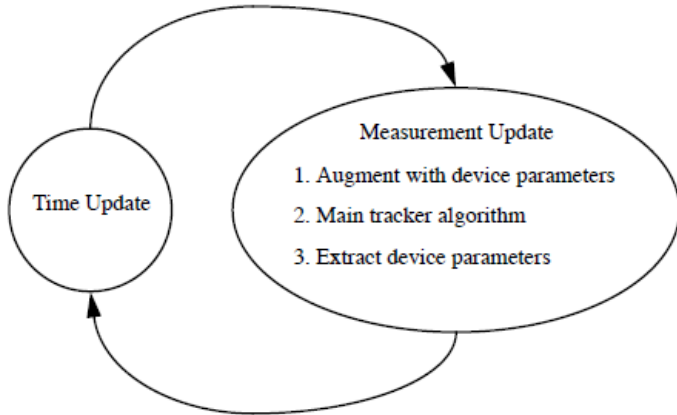
**Figure 4.9:** Geometric view of state change after measurement correction. Per the information in the measurement residual, the *a posteriori* state estimate is formed, i.e. the estimated target coordinate frame is moved and reoriented. Compare this with figure 4.2 on page 85. (Again the derivative elements of the state have been omitted and the spacial relationship exaggerated for clarity.)



**Figure 4.10:** Geometric view of error covariance change after measurement update. The change is shown by a refined probability density for each of  $x$ ,  $y$ , and  $z$ . Note that in general the density is reoriented to reflect the constraint provided by the measurement. Compare this with figure 4.3 on page 85. (Again to visualize with Euclidean dimensions, the density has been limited to 3D:  $x$ ,  $y$ , and  $z$  only. The absolute shape, magnitude, and orientation are illustrative only.)

Welch Thesis at 95.

## Exhibit D-21

CLAIM 60	Welch Thesis
	 <p><b>Figure 4.12:</b> The revised tracking algorithm for autocalibration. The time update consists of equation (4.14). The measurement update consists of equations (4.24)-(4.27), then (4.15)-(4.22), and finally equation (4.28).</p> <p>Welch Thesis at 102.</p> <p>The Kalman filter estimates a process by using a form of feedback control: the filter estimates the process state at some time and then obtains feedback in the form of (noisy) measurements. As such, the equations for the Kalman filter fall into two groups: time update equations and measurement update equations. The time update equations are responsible for projecting forward (in time) the current state and error covariance estimates to obtain the a priori estimates for the next time step. The measurement update equations are responsible for the feedback—i.e. for incorporating a new measurement into the a priori estimate to obtain an improved a posteriori estimate. The time update equations can also be thought of as predictor equations, while the measurement update equations can be thought of as corrector equations. Indeed the final estimation algorithm resembles that of a predictor-corrector algorithm for solving numerical problems as shown in figure B.1.</p> <p>Welch Thesis at 170-71.</p>

## Exhibit D-21

CLAIM 60	Welch Thesis
	<div data-bbox="739 246 1159 555" data-label="Diagram"> <pre> graph LR     A((Time Update ("Predict"))) --&gt; B((Measurement Update ("Correct")))     B --&gt; A </pre> </div> <p data-bbox="562 607 1360 727"><b>Figure B.1:</b> The ongoing discrete Kalman filter cycle. The <i>time update</i> projects the current state estimate ahead in time. The <i>measurement update</i> adjusts the projected estimate by an actual measurement at that time. Notice the resemblance to a <i>predictor-corrector</i> algorithm</p> <p data-bbox="514 740 785 773">Welch Thesis at 171.</p> <p data-bbox="514 808 1953 1243">To use Powell’s method, I needed to define a cost function that returned a scalar indication of the “goodness” of a particular set of parameters. In simulations I had access to both the estimated filter state and the “true” state (see “Motion Bandwidth” below) for several motion data sets as described in section E.1. Again employing a scheme similar to that of Azuma and Bishop, I designed a special simulation framework for the purpose of parameter optimization. At every filter update step <b>I compute the locations (in world coordinates) of three points arranged in a triangle that is oriented upright and faces the HiBall approximately one meter in front of the HiBall.</b> I compute these three points for both the estimated filter state and the true state, and then I compute the average distance between the respective estimated and true point groups. This average distance provides a per-estimate scalar cost, which I then average for an entire simulation run (for a particular data set) to obtain the necessary scalar cost for a particular parameter set <math>P[N]</math>. This approach nicely combines position and orientation error into a single cost. The parameters found using this method for various test cases are given in section 6.2.1 of chapter 6.</p> <p data-bbox="514 1247 777 1279">Welch Thesis at 198</p> <p data-bbox="514 1315 1969 1422"><i>See also</i> Welch Thesis Chapter 2.5 (describing autocalibration for sensor subsystems); Chapter 3.2 (describing sequential estimate updates performed by the SCAAT algorithm as new measurement data is collected by the system); Chapter 4.3 (use of the SCAAT algorithm for tracking to predict and correct sensor measurements);</p>

## Exhibit D-21

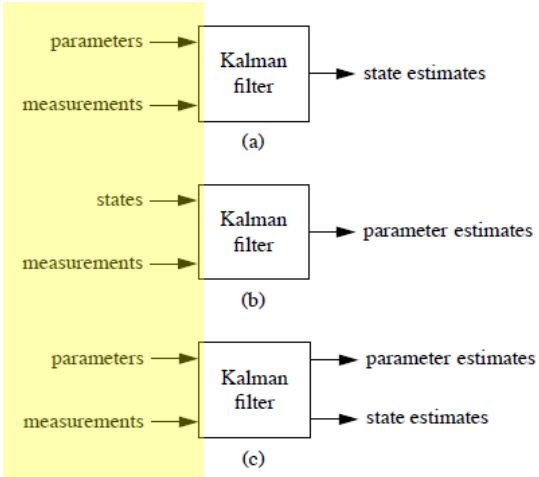
CLAIM 60	Welch Thesis
	<p>Chapter 4.4 (autocalibration using SCAAT algorithm); Chapter 6.1 (describing autocalibration of HiBall sensor system using SCAAT)</p> <p><i>See also</i> Defendants' Invalidity Contentions for further discussion.</p>

**R. DEPENDENT CLAIM 61**

CLAIM 61	Welch Thesis
<p>[61] The method of claim 47 wherein providing configuration information from the sensor modules includes providing information characterizing one or more calibration parameters of a sensor associated with a sensor module.</p>	<p>At least under Plaintiffs' apparent infringement theory, Welch Thesis discloses, either expressly or inherently, the method of claim 47 wherein providing configuration information from the sensor modules includes providing information characterizing one or more calibration parameters of a sensor associated with a sensor module. In the alternative, this element would be obvious over Welch Thesis in light of the other references disclosed in Defendants' Invalidity Contentions and/or the knowledge of one of ordinary skill in the art.</p> <p><i>See, e.g.:</i></p>



## Exhibit D-21

CLAIM 61	Welch Thesis
	 <p data-bbox="541 722 1180 873"><b>Figure 2.2: State versus parameter estimation.</b> (a) The system parameters are known, and are used with the measurements to estimate the states. (b) For calibration purposes, known states can be used with measurements to estimate the system parameters. (c) A set of parameters can be used in conjunction with measurements to estimate another (not necessarily disjoint) set of parameters <i>and</i> the states.</p> <p data-bbox="514 898 768 930">Welch Thesis at 49.</p>

## Exhibit D-21

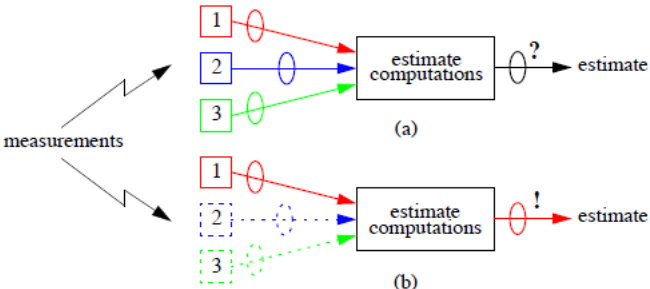
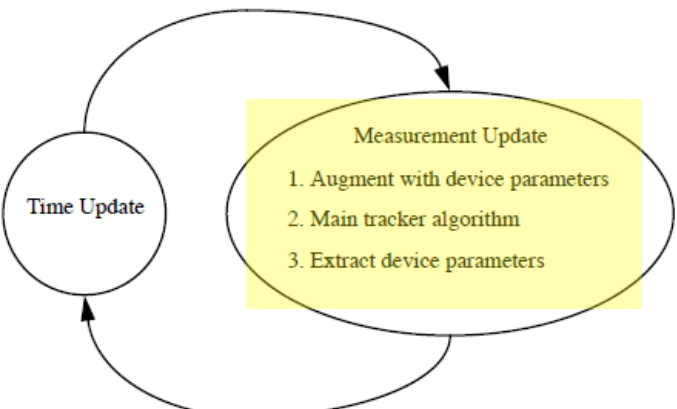
CLAIM 61	Welch Thesis
	 <p><b>Figure 2.11:</b> Autocalibration and attribution of measurement error. (a) Most algorithms operate on multiple measurements as a group, hence uncertainty or error (represented by the ellipses) in the final estimates is difficult to attribute to any individual sensor. (b) With the SCAAT method, uncertainty in final estimates can more easily be attributed to a particular individual sensor.</p> <p>Welch Thesis at 62.</p>  <p><b>Figure 4.12:</b> The revised tracking algorithm for autocalibration. The time update consists of equation (4.14). The measurement update consists of equations (4.24)-(4.27), then (4.15)-(4.22), and finally equation (4.28).</p> <p>Welch Thesis at 102.</p> <p>See also Welch Thesis Chapter 2.5 (describing autocalibration for sensor subsystems); Chapter 4.4 (autocalibration using SCAAT algorithm); Chapter 6.1 (describing autocalibration of HiBall sensor system using SCAAT)</p>

Exhibit D-21

CLAIM 61	Welch Thesis
	<i>See also</i> Defendants' Invalidity Contentions for further discussion.